ORIGINAL RESEARCH
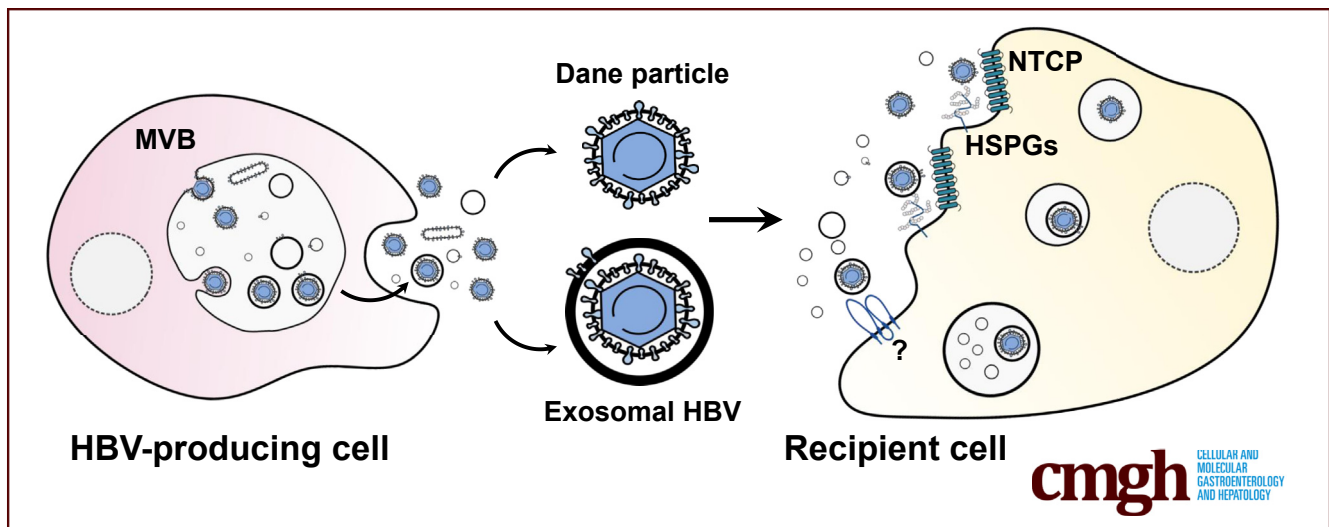
Presence of Intact Hepatitis B Virions in Exosomes

Qingyan Wu,[1] Mirco Glitscher,[1] Susanne Tonnemacher,[2] Anja Schollmeier,[1] Jan Raupach,[1] Tobias Zahn,[1] Regina Eberle,[2] Jacomine Krijnse-Locker,[2] Michael Basic,[1,3] and Eberhard Hildt[1,4]

[1]Department of Virology, Paul-Ehrlich-Institute, Langen, Germany; [2]Loewe Center DRUID, Paul-Ehrlich-Institute, Langen, Germany; [3]Department of Gastroenterology and Hepatology, University Hospital Frankfurt, Frankfurt, Germany; and [4]German Center of Infection Research (DZIF), Gießen-Marburg-Langen, Germany

SUMMARY

A so-far unreported virion egress pathway of hepatitis B virus was identified. The presence of intact virions in exosomes was visualized for the first time. Exosomes hijacked by hepatitis B virus act as a transporter impacting the spread of the virus.

BACKGROUND & AIMS: Hepatitis B virus (HBV) was identified as an enveloped DNA virus with a diameter of 42 nm. Multivesicular bodies play a central role in HBV egress and exosome biogenesis. In light of this, it was studied whether intact virions wrapped in exosomes are released by HBV-producing cells.

METHODS: Robust methods for efficient separation of exosomes from virions were established. Exosomes were subjected to limited detergent treatment for release of viral particles. Electron microscopy of immunogold labeled ultrathin sections of purified exosomes was performed for characterization of exosomal HBV. Exosome formation/release was affected by inhibitors or Crispr/Cas-mediated gene silencing. Infectivity/

uptake of exosomal HBV was investigated in susceptible and non-susceptible cells.

RESULTS: Exosomes could be isolated from supernatants of HBV-producing cells, which are characterized by the presence of exosomal and HBV markers. These exosomal fractions could be separated from the fractions containing free virions. Limited detergent treatment of exosomes causes stepwise release of intact HBV virions and naked capsids. Inhibition of exosome morphogenesis impairs the release of exosome-wrapped HBV. Electron microscopy confirmed the presence of intact virions in exosomes. Moreover, the presence of large hepatitis B virus surface antigen on the surface of exosomes derived from HBV expressing cells was observed, which conferred exosome-encapsulated HBV initiating infection in susceptible cells in a , large hepatitis B virus surface antigen/Na^+–taurocholate co-transporting polypeptide-dependent manner. The uptake of exosomal HBV with low efficiency was also observed in non-permissive cells.

CONCLUSION: These data indicate that a fraction of intact HBV virions can be released as exosomes. This reveals a so far not described release pathway for HBV. *(Cell Mol Gastroenterol*

Hepatitis B virus (HBV) is a small, enveloped DNA virus and belongs to the family of Hepadnaviridae. The HBV virion is a spherical particle with a diameter of 42 nm. The outer envelope, which harbors the three viral surface proteins large hepatitis B virus surface antigen (LHBs), middle hepatitis B virus surface antigen (MHBs), and small hepatitis B virus surface antigen (SHBs), surrounds the nucleocapsid. The entirety of all HBV surface proteins are designated as HBsAg. The icosahedral nucleocapsid is formed by the core protein (HBcAg) and harbors the partial double-stranded DNA genome of about 3.2 kb. The HBV genome encompasses 4 open reading frames encoding for the viral polymerase, for the core antigen (HBcAg) or its secretory variant e antigen (HBeAg), for the surface proteins (HBsAg) and for the regulatory X protein.[1,2]

In addition to infectious viral particles, HBV-producing cells release non-infectious subviral particles which are exclusively formed by HBsAg and lack a genome and any other HBV protein. Two forms can be distinguished, 22 nm sized spheres and long filaments. Although the spheres are mainly assembled by SHBs and contain only smaller amounts of LHBs and MHBs, the filaments are characterized by a higher LHBs content. In addition, naked capsids lacking the envelope are released.[3-6]

Infection with HBV can cause acute and chronic hepatitis. Serological evidence indicates that past or present infection exists in more than 2 billion individuals all over the world.[7] There are approximately 1.5 million new infections each year worldwide.[8] In 2019, an estimated 296 million people suffered from chronic infection.[9] Chronic HBV infection is associated with an increased risk to develop cirrhosis or hepatocellular carcinoma. More than 620,000 people annually die from the consequences of HBV infection.[10] Although safe and effective vaccines are licensed, HBV continues to be a major health problem, as in many countries with a high epidemic burden no effective vaccination strategies are in place. Moreover, the complete cure of an established chronic infection is far from being solved.[2,11]

During the past 50 years, essential principles of HBV entry life cycle and morphogenesis have been revealed. Growing evidence indicates that the egress of virions and of the subviral filaments depends on the endosomal sorting complexes required for transport (ESCRT) machinery and host intracellular vesicle trafficking pathways.[3,12-14] In contrast to this, spheres are secreted by the classic secretory pathway.[15,16] The current studies also reveal that HBV envelope proteins can be trafficked from the ER/Golgi complex to the endosomal system and ultimately to the membranes of multivesicular bodies.[17-19] For HBV release from the host cell, multivesicular bodies (MVBs) are assumed to be the platform for HBV budding and egress. Here, mature nucleocapsids are enveloped by the viral surface proteins and then are released from cells by means of the exosomal pathway as the MVBs fuse with the plasma membrane. The pathway of exosome formation overlaps significantly with the morphogenesis of HBV. Exosomes are generated by the MVBs harboring intraluminal vesicles.[20] This implies that the budding of HBV is intimately intertwined with the biogenesis of exosomes.

Numerous studies have shown that both enveloped and non-enveloped viruses can be found within exosomes. This affects cell-to-cell spread and viral immune evasion.[21,22] Biochemical analyses reveals that the prototypic non-enveloped hepatitis A and hepatitis E viruses are released from the infected cells as "quasi-enveloped virus" by cloaking itself completely within membranes that resemble exosomes.[23-26] Similarly, in vitro productive hepatitis C virus (HCV) transmission can be caused by exosomes released from HCV-infected hepatoma cells.[27] Furthermore, several studies indicated that exosomes released by human immunodeficiency virus (HIV)-infected cells affect the infection process by containing HIV-derived virulence factors.[28-30] Unlike HCV or HIV, there is no evidence for the presence of viral antigens on the surface of these quasi-enveloped infectious hepatitis A virus (HAV) and only ambiguous evidence in case of hepatitis E virus.[23-26] The similarity of exosome biogenesis with HBV egress pathways raises the question whether complete HBV progeny virions usurp the exosome biogenesis machinery for dissemination.

Generally, exosomes are small vesicles in the size range of 30 to 150 nm with buoyant density in certain media from 1.08 to 1.20 g/cm^3,[31,32] which is similar to the density of many viral particles. The process of exosome enrichment based on differential ultracentrifugation actually co-precipitates many viral particles in parallel.[22] Therefore, a more efficient separation method is needed to study their respective functions. In this study, we demonstrated that exosomes and HBV virions can be sufficiently separated on the basis of their different sedimentation in an iodixanol gradient, which has also been used for separation of exosomes from HIV particles[33,34] and enveloped viruses

('eHAV') from picornaviruses.[23] This enabled us to perform an in-depth analysis of exosomal cargoes. We observed that complete HBV virions are encapsulated in these highly purified exosomes and detected the infectivity of these exosomal viruses by infection of differentiated HepaRG cells. Thus, our study reveals an undiscovered pathway for HBV release, namely utilizing the exosomal route to spread host membrane-entrapped HBV particles.

Results

Presence of HBV-specific DNA and Viral Proteins in Exosomes Released From HBV-expressing Cells

To shed light on the potential role of exosomes for the release and spread of HBV, the characteristics of exosomes purified from the culture fluids of human hepatoma cell lines were systematically analyzed. Using differential ultracentrifugation, exosomes were pelleted from supernatant of HBV-negative HepG2 cells or of the HBV-expressing stable cell line HepAD38 (Figure 1, A). To analyze the size distribution of exosomes derived from these 2 sources, nanoparticle tracking analysis (NTA) was performed. The NTA revealed a significant difference between HepG2- and HepAD38-derived exosomes. The peak diameter of exosomes from HepAD38 cell-derived exosomes was around 134 nm. In case of HepG2 cell-derived exosomes, the peak diameter was at 119 nm (Figure 1, B).

Many approaches for exosome isolation are based on a differential centrifugation step. However, the similarity of sedimentation properties of exosomes and HBV virions causes a co-sedimentation of exosomes and HBV virions. Therefore, the purification procedure was extended by an iodixanol density gradient centrifugation method to efficiently separate exosomes from virions (Figure 1, A). Western blot analyses using exosome- and HBV-specific markers revealed that there were core and LHBs containing fractions at higher gradient densities, which were separated from the fractions identified as exosomes characterized by the markers Alix, Tsg101, and CD63 (Figure 1, C).

Analysis of the viral DNA and HBcAg distribution over the gradient revealed 2 peaks. There was an HBV-DNA and core-positive peak at lower density, encompassing fractions 6 to 9 (corresponding to a density of 1.06–1.10 g/cm^3), which were characterized by the presence of the exosomal markers (Figure 1, D).

The second HBV-DNA- and HBcAg-positive peak appeared at the expected density of HBV virions in fraction 12 (corresponding to a density of 1.18 g/cm^3) and was further characterized by the absence of exosomal markers (Figure 1, D).

As the exosomal fractions were HBcAg-positive, it was further analyzed if these fractions were HBsAg-positive, too. For this purpose, the untreated fractions and radio-immunoprecipitation assay (RIPA) buffer pretreated fractions were analyzed by HBsAg-specific enzyme-linked immunosorbent assay (ELISA). RIPA buffer was used to destroy exosomal membranes. The ELISA revealed that in fractions F5 to F7, which were characterized by the exosomal markers, the RIPA buffer treatment caused a significant increase of the HBsAg signal (Figure 1, E). This indicates that destruction of the exosomal membrane makes the HBsAg cloaked within exosomes accessible for the detection by the HBsAg-specific antibodies.

To further confirm the presence of LHBs and HBcAg within the exosomes, immunoprecipitations (IPs) were performed. The exosomal fractions isolated as shown in Figure 1, A were subjected to precipitation with CD63-coated magnetic beads. The input, unbound supernatant after IP, and the bead-bound exosomes were evaluated by Western blotting (Figure 1, F). As compared with the input, a significant decrease in Alix, LHBs, and HBcAg levels was observed in the unbound supernatants (Figure 1, F). Meanwhile, the presence of Alix, LHBs, and HBcAg was detected in the bead-bound exosomes after IP of the exosomal inputs with CD63-coated magnetic beads (Figure 1, F).

IP of exosomal fractions with an unrelated Dynabead sheep anti-rabbit immunoglobulin G (IgG) showed that there was no detectable HBV antigen signal or exosomal marker Alix precipitated by the control magnetic beads, and the weak LHBs signal in the precipitates is probably derived from non-specific binding or residual subviral particles (Figure 1, F). These data indicate that there is a co-existence of LHBs and HBcAg within the exosomes.

Quantification of HBV genomic DNA by quantitative polymerase chain reaction (qPCR) and HBcAg by ELISA in the exosomal fractions revealed that the percentage of exosome-associated HBV genomic DNA and HBcAg referred to the total input of the gradient were approximately 1.76% and 2.04%, respectively (Figure 1, G).

Taken together, these results indicate that HBV-expressing cell line releases exosomes that can be efficiently separated from free virions. Moreover, in the exosomal fractions, HBcAg, LHBs, SHBs, and viral DNA are detectable.

Detection of Viral Particles in Exosomes Derived From HBV-expressing Cells

The data described above indicate that, in exosomes isolated from HBV-expressing cells viral DNA, HBsAg, and HBcAg can be detected. Meanwhile, anti-CD63 immunogold labeling and negative staining further confirmed that exosome population was present in the lower density peak (Figure 2, A). In contrast, only HBV virions were observed in the second HBV-DNA- and HBcAg-positive peak shown in Figure 1, D, where they exhibited a typical negative staining structure, which was also confirmed by the anti-preS1/preS2 immunogold labeling (Figure 2, B). This then begs the question of whether fully assembled virions can be found within the exosomes. To investigate this, exosomal fractions (fractions 6 to 9) were isolated as described above and treated with 0.5% nonyl phenoxypolyethoxylethanol (NP-40) for 2 hours at 37 °C and again subjected to iodixanol density gradient centrifugation. Untreated exosomes served as control (Figure 2, C). Quantification of the viral

DNA over the gradient fractions confirmed for the untreated input the presence of viral DNA in fractions 7 to 9, corresponding to a density of 1.064 to 1.105 g/cm^3 (Figure 2, D).

In the NP-40-treated input, the viral DNA was shifted to fractions 11 to 14 with a density of 1.185 g/cm^3 for the peak fraction (fraction 12) (Figure 2, D).
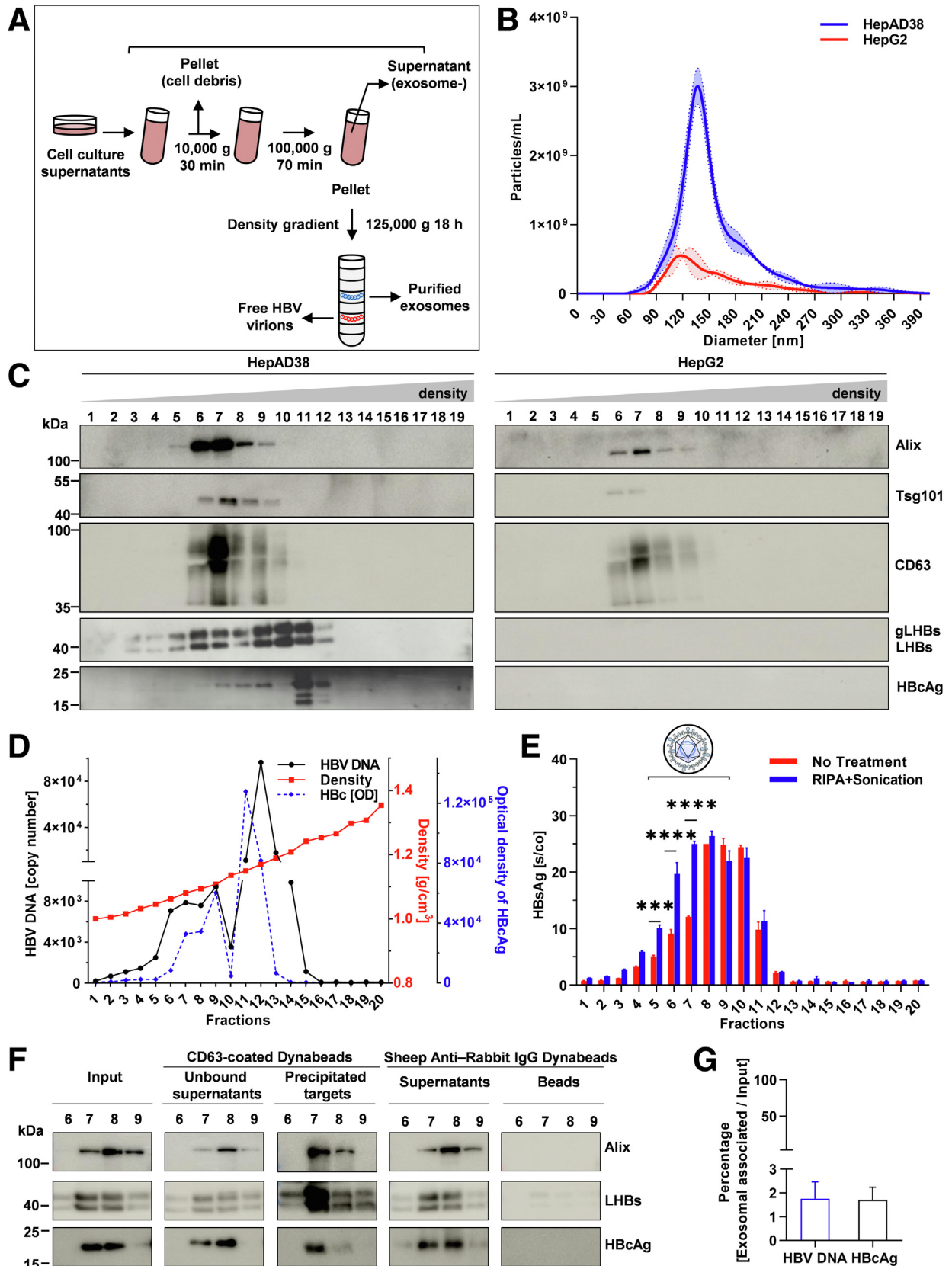
The fractions derived from the iodixanol gradients of the untreated and the NP-40-treated input were analyzed by Western blot. The Western blot analysis revealed that, in the untreated samples, the exosomal markers, LHBs, and HBcAg were concentrated in fractions 7 to 9 (Figure 2, E). In case of the NP-40-treated input, there was a shift of the HBcAg-containing fractions to a higher density (1.185 g/cm^3) (Figure 2, E). This might represent a mixture of free virions and naked capsids, which are generated by the detergent-dependent destruction of the exosomal membrane and virus envelope. This is corroborated by the shift of the LHBs containing fractions to lower densities reflecting the membrane destruction as shown in Figure 2, E. Moreover, the fraction 8 (in case of the untreated input) and the fractions 11 and 12 (in case of the NP-40-treated input) of the gradient were analyzed by an HBcAg-specific ELISA. The ELISA revealed significant lower values for fraction 8 (untreated input) as compared with fractions 11 and 12 (NP-40-treated input) (Figure 2, F). Here, the intensive NP-40 treatment has stripped of the masking exosomal and viral membrane. Thereby, the capsid becomes accessible for the core-specific antiserum. When fraction 8 (untreated input) is treated with Triton X-100, which causes destruction of the exosomal and viral membrane, a significant higher HBcAg-specific signal is obtained (Figure 2, F).

These data indicate that viral particles can be found in the exosomal fractions. Destruction of the exosomal membrane by mild detergent is associated with partial destruction of the viral envelope.

Exosomes Derived From HBV-producing Cells Harbor Intact HBV Virions

Mild detergent treatment of exosomes causes the release of HBV-DNA-containing particles, which might represent a mixture of viral particles and naked capsids. To investigate if naked capsids and intact HBV virions can be separated by iodixanol gradient centrifugation, purified virions and purified virions treated with NP-40 were subjected to iodixanol density gradient centrifugation. The fractions were analyzed by qPCR for quantification of the viral DNA. As shown in Figure 3, A, there is no significant difference in the distribution over the gradient between intact virions and NP-40-treated virions. In both cases, there is a peak for the viral DNA corresponding to a density of about 1.18 to 1.20 g/cm^3. However, if purified virions and NP-40-treated purified virions were loaded on a sucrose gradient and the fractions were analyzed by qPCR, a clear separation of the virion-specific peak from the naked capsid-specific peak was obtained (Figure 3, B). This was further confirmed by analysis of the respective peak fractions of the sucrose gradient fraction 12 (untreated) and fraction 15 (NP-40-treated) by HBcAg ELISA (Figure 3, C). In case of fraction 12, a significant lower HBcAg-specific signal was observed as compared with fraction 15, although in both fractions, comparable numbers of HBV genomes were detected (Figure 3, B). However, when fraction 12 was treated with Triton X-100 to remove the protecting viral envelope, the HBcAg-specific signal was drastically increased (Figure 3, C). These data indicate that under these conditions naked capsids can be efficiently separated from intact virions.

Therefore, this sucrose gradient system was used to analyze the exosomal fraction (fraction 8), which was obtained from the iodixanol gradient (Figure 2, D). One-half of the fraction was left untreated; the other half was subjected to a limited NP-40 treatment (0.25% NP-40, 20 minutes at 30 °C) (Figure 3, D). The fractions of the sucrose gradient were analyzed by qPCR for quantification of HBV genomes. The qPCR revealed for the untreated exosomal fraction after sucrose gradient centrifugation one peak (fractions 7–9) (Figure 3, D). For the NP-40-treated exosomal fraction, a clear separation of virions (fraction 11, 12) and naked capsids (fraction 14, 15) by the sucrose density gradient was observed (Figure 3, D). At the same time, by negative staining and transmission electron microscopy, HBV virions were observed in fractions 11 and 12, which were enriched by ultracentrifugation (Figure 3, E). Moreover, the fractions of the sucrose gradient (Figure 3, D) were analyzed by Western blot. In case of the untreated input, detection of Alix as exosomal marker confirmed the presence of exosomes in fractions 7 to 9 (Figure 3, F). In the same fractions, HBcAg was found, and the strongest LHBs-specific signal was obtained. The respective analysis of the NP-40-treated input revealed that the Alix-specific signal almost diffused over the entire

Figure 1. (*See previous page*). **Isolation and characterization of exosomes purified from human hepatoma cell lines.** *A*, Schematic description of the exosome purification procedure from the culture fluids of human hepatoma cell lines. *B*, The size distribution of exosomes isolated from HBV-negative HepG2 cells and from the HBV-expressing stable cell line HepAD38. Analysis of size distribution was performed by NanoSight NS300. The error bars were shown as dotted lines with fill areas. *C*, Exosomes were isolated from the supernatant of HepAD38 (*left*) or HepG2 cells (*right*) as shown in Figure 1, *A* by differential centrifugation followed by iodixanol density gradient centrifugation. The fractions of the iodixanol gradient were analyzed by Western blot detecting Alix, Tsg101, and CD63 as exosomal markers and LHBs and HBcAg as HBV components. *D*, Absolute quantification of the distribution of HBV genomes (*black line*) and of HBcAg (quantification of the Western blot in Figure 1, *C*) (*blue dotted line*) in each fraction in the iodixanol gradient. The density is shown by the *red line*. *E*, Quantification of HBsAg in each fraction in the iodixanol gradient by ELISA. The fractions were either left untreated (*red bars*) or pretreated with RIPA buffer and ultrasound sonication (**blue bars**). Two-way analysis of variance followed by the Sidak multiple comparison test for all panels. ***$P < .001$. *F*, IP assay of the exosomal iodixanol gradient fractions with CD63-coated magnetic beads or unrelated Dynabeads M-280 Sheep Anti–Rabbit IgG as control. The input, unbound supernatants, and immunoprecipitated targets from the fractions were analyzed by Western blot, detecting Alix as exosomal marker and LHBs and HBcAg as HBV components. *G*, The percentage of exosome-associated HBV genomic DNA and exosomal-associated HBcAg as compared with the total input supernatant. HBV genomic DNA in the exosomal fractions and in the input of the gradient was quantified by qPCR. Quantification of HBcAg was performed by HBcAg-specific ELISA.

gradient, and the core-specific signal was shifted to fractions 10 to 12 and 14 to 16 (Figure 3, *F*). The LHBs-specific signal smeared over fractions 2 to 14 under these conditions due to the destruction of membranes.

Analysis by an HBcAg-specific ELISA revealed that for fraction 8 and 11, 12 of the gradient shown in Figure 3, *D*, addition of Triton X-100 pretreatment caused a strong increase of the HBcAg-specific signal (Figure 3, *G*). This
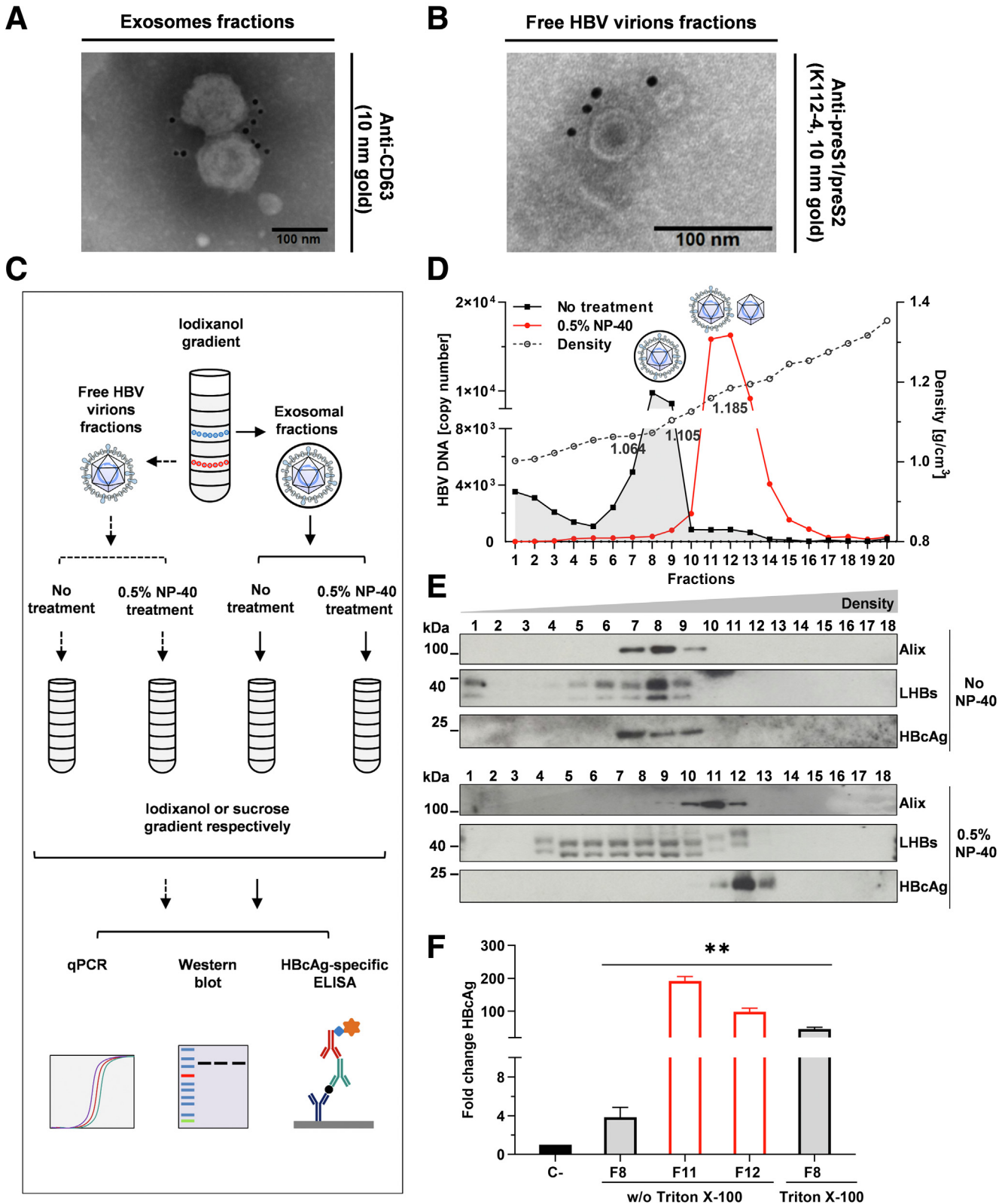
reflects that, due to the Triton X-100 treatment, the exosomal and viral membranes were removed, and the core became accessible for detection by the HBcAg-specific antibody.

After increasing the NP-40 treatment concentration to 0.5% and treating at 37 °C for more than 1 hour, the qPCR revealed for the NP-40-treated input, the viral DNA was completely shifted to the naked capsid fraction (fraction 15) (Figure 3, H). Moreover, the core-specific signal was shifted to the same fractions as the envelope of all intact HBV virions, which were released by the destruction of the exosomes was removed (Figure 3, H). The naked capsid fractions 14 and 15 of the sucrose gradient (NP-40-treated) in Figure 3, H, and the naked capsid fraction 15 of the sucrose gradient (NP-40-treated) in Figure 3, D were also analyzed by transmission electron microscopy (TEM). By negative staining, only naked capsids without any HBV envelope were observed in these fractions (Figure 3, I).

Taken together, based on a sucrose gradient, it was demonstrated that after mild and limited NP-40 treatment, intact virions can be released from exosomes and separated from naked capsids. These data further confirm the presence of intact viral particles in the exosomal fraction.

Interference With MVB or Exosome Formation by Specific Inhibitors Affects the Release of Encapsulated HBV

The data described above indicate that intact HBV virions can be found in exosomes. To study the impact of interference with MVB functionality and exosome biogenesis on the release of encapsulated HBV, various inhibitors were used.

U18666A inhibits directly NPC1/2 protein and thereby impairs the intracellular trafficking of cholesterol. This causes dysfunction of MVBs and consequently affects the release of exosomes.[35] HepAD38 cells were incubated for 48 hours with 2 or 4 μg/mL U18666A. The supernatant was analyzed as described above (Figure 1, A). The fractions of the iodixanol gradient were analyzed by HBV-specific qPCR for quantification of the viral genomes (Figure 4, A) and by Western blot analysis using Alix-specific and core-specific antibodies (Figure 4, B). As compared with the untreated control, the U18666A treatment changed the distribution of Alix (Figure 4, B). The amount of Alix and Tsg101 in the

exosomal fractions (fractions 6–8) was decreased after U18666A treatment (Figure 4, B). The viral DNA (Figure 4, A) and HBcAg (Figure 4, B) almost completely disappeared from fractions 6 to 8 after U18666A treatment and were concentrated in fractions 10 and 12 (viral DNA) and in fraction 10/11 (HBcAg).

Comparable results were obtained using manumycin A (Figure 4, C), which inhibits the ESCRT-dependent exosome biogenesis, and GW4869 (Figure 4, D), which impairs exosome release by inhibition of neutral sphingomyelinases (nSMase). In both cases, the number of HBV genomes in the exosomal fraction was dose-dependently reduced (Figure 4,C–D). The effectiveness of manumycin A or GW4869 treatment on exosome formation was controlled by analyzing the distribution of Alix in the exosomal fractions (Figure 4, E). The amount of Alix in the exosomal fractions was decreased in both cases (Figure 4, E).

To further confirm that the observed inhibition of the formation of exosome-coated HBV is caused by impairment of exosome formation specificity, the influence of these inhibitors on HBV replication and HBsAg production was studied by Western blot for quantification of intracellular LHBs and HBcAg (Figure 4, F–G), by qPCR for the levels of intracellular HBV total RNAs (Figure 4, H) and by ELISA for the extracellular levels of HBsAg and HBeAg (Figure 4, I). As compared with the untreated cells, almost the same amount of intracellular LHBs and HBcAg was observed in the groups of cells treated with different inhibitors for 48 hours (Figure 4, G). In addition, there was no great difference in the amount of intracellular HBV total RNAs (Figure 4, H) and in the extracellular levels of HBeAg (Figure 4, I, lower panel) between the inhibitor-treated and untreated cells. In manumycin A- or GW4869-treated cells, the release of HBsAg (extracellular) was also not impacted (Figure 4, I, upper panel). However, the release of HBsAg was significantly reduced by both concentrations in U18666A-treated cells (Figure 4, I, upper panel), which was also observed in a previous study.[14] It was mainly caused by the effect of U18666A on the formation of MVBs, which is the platform for the release of both HBV virions and HBV subviral filaments. However, as shown in Figure 4, A, the number of HBV genomes in fraction 12 (free virions) was not significantly decreased by U18666A treatment, and intracellular LHBs showed no significant accumulation (Figure 4, G). Therefore, most of the diminution of extracellular HBsAg observed in

Figure 2. (See previous page). Separation of exosomal HBV and free HBV by iodixanol- and sucrose-density centrifugation. *A*, Immunogold labeling of exosomal fractions from the iodixanol gradient as shown in Figure 1, *A* was visualized by phosphotungstic acid negative staining with an anti-CD63 antibody (10 nm gold). *B*, Immunogold phosphotungstic acid staining the HBV virions fraction from the iodixanol gradient as shown in Figure 1, *A* using an anti-preS1/preS2 domain rabbit serum (K112-4, 10 nm gold). *C*, Schematic description: exosomal fractions 7 to 9 or free HBV virions fractions of the iodixanol gradient were pooled. One-half was left untreated; the other half was adjusted to 0.5% NP-40 and incubated for 2 hours at 37 °C. Subsequently, re-centrifugation on an iodixanol or sucrose density gradient was performed. *D*, Absolute quantification of the distribution of HBV genomes by qPCR in each fraction in the iodixanol gradient. The untreated input is represented by the *black line*. The NP-40-treated input is represented by the *red line*. The density is shown by the *gray line*. *E*, Western blot analysis of the fractions of the iodixanol gradient centrifugation of the untreated input and of the NP-40-treated input. For detection, the LHBs- and core-specific antibodies and the Alix-specific antibody were instrumental. *F*, Quantification of HBcAg was performed by HBcAg-specific ELISA in fraction 8 (NP-40-untreated input) and fractions 11, 12 (NP-40-treated input) of the iodixanol gradients (Figure 2, *D*) in the presence or absence of Triton X-100 detergent. Unpaired parametric *t* tests for all panels; **$P < .01$.

U18666A-treated cells probably resulted from the reduced release of HBV subviral filaments, because, compared with the amount of released viral particles, HBV-infected cells have a tendency to release a higher amount of subviral particles. Accordingly, these data show that comparable HBV replication and HBsAg production were observed in cells in the
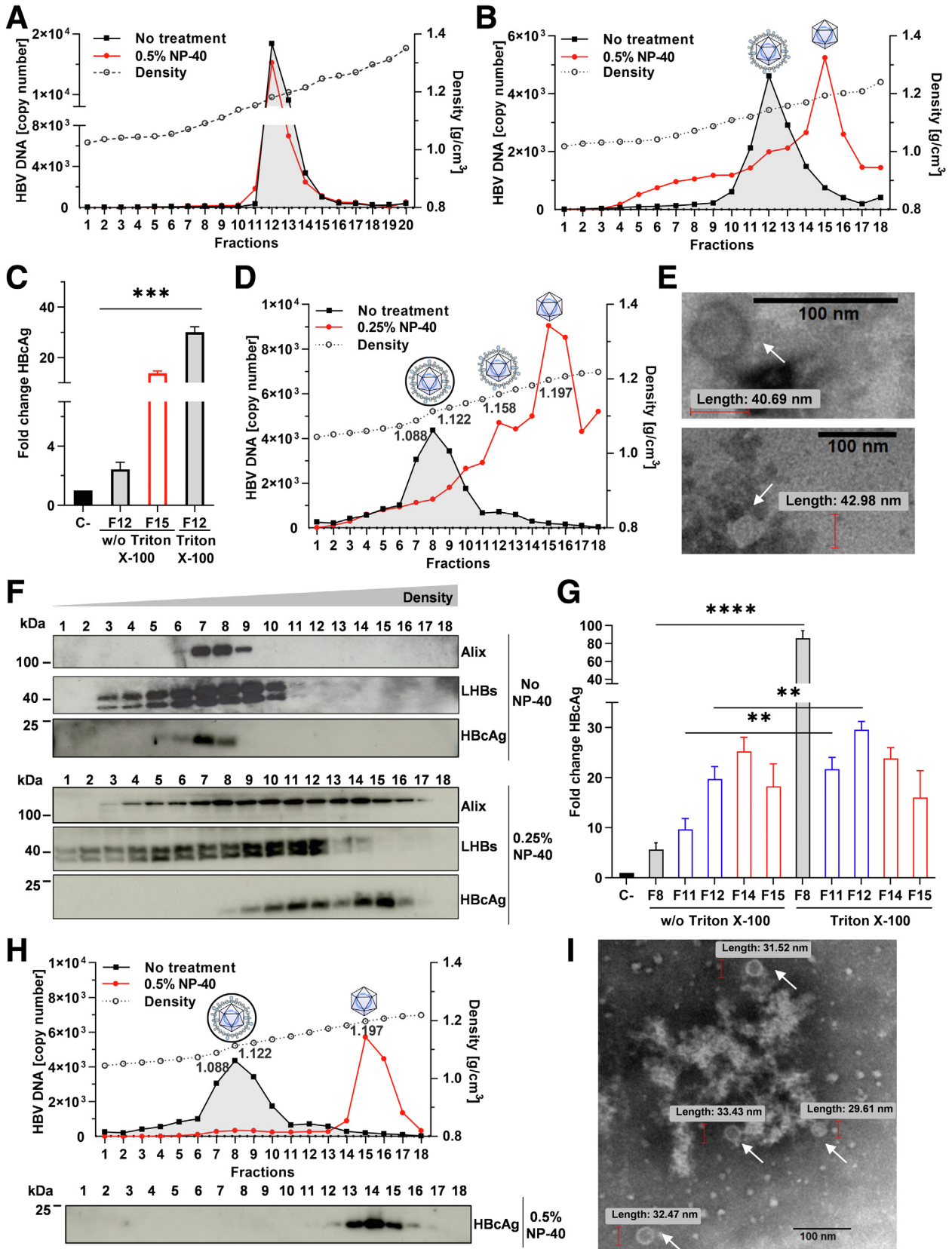
presence of manumycin A or GW4869 inhibitors compared with untreated cells. In U18666A-treated cells (Figure 4, A), comparable amounts of viral genomes were also detected in the gradient compared with the untreated group.

Thus, these data indicate that inhibition of exosome biogenesis/release with these inhibitors specifically impairs the release of membrane-cloaked HBV virions.

Release of Host Membrane-cloaked HBV Particles Requires Exosome-associated Proteins

The experiments described above demonstrate that MVBs and exosomes play an important role in mediating the maturation and trafficking of host membrane-cloaked HBV. To clarify the mechanism by which HBV enters exosomes, specific proteins with key roles in exosome biogenesis and in MVBs/exosome cargo sorting were targeted. Several lines of evidence indicate that ESCRT-associated protein Alix (PDCD6IP) mediates the biogenesis of host membrane-cloaked virions.[23,36,37] To assess the direct impact of Alix on release of the exosomal HBV particles, an Alix-deficient HepAD38 cell line was generated (Alix-knockout [KO]), using CRISPR/Cas9 mutagenesis. Loss of endogenous Alix protein was confirmed by Western blotting of cellular lysates derived from Alix-KO cells (Figure 5, A). In parallel, HBV replication and HBsAg production were investigated in Alix-deficient HepAD38 cell lines. Western blot analysis for detection of the intracellular LHBs showed a lower amount of N-glycosylated species of LHBs in these cell lines as compared with the non-target (NT) cells (Figure 5, C), but the levels of intracellular HBcAg remained unchanged (Figure 5, C). Quantification of intracellular HBV total RNAs displayed for the Alix-deficient HepAD38 cells a comparable amount of HBV total RNAs as compared with the NT cells (Figure 5, D). Analysis of the levels of HBV genomic DNA in the supernatants by qPCR revealed a decreased HBV release in the Alix-KO cell lines as compared with NT cells (Figure 5, E). Detection of

extracellular HBsAg and HBeAg levels by ELISA showed that the same levels of HBsAg and HBeAg were released in the Alix-deficient cells compared with the NT cells (Figure 5, F–G).

Subsequently, the supernatant of these cell lines was subjected to differential centrifugation followed by iodixanol-gradient as schematically shown in Figure 1, A. HBV genome distributions in iodixanol density gradient of Alix-deficient HepAD38 cells and NT cells were quantified by qPCR (Figure 5, H). As the release of HBV was slightly affected (Figure 5, E) and the amount of HBV-DNA in both the exosomal fractions and the free HBV virions fractions was reduced in Alix-deficient HepAD38 cell lines as compared with the NT cells (Figure 5, H). The fold change for each fraction referred to fraction 12 (HBV virions fraction) was analyzed and is shown in Figure 5, I. Analysis of the gradients by qPCR for quantification of the viral genomes revealed that for the exosomal peak (fractions 6, 7) the number of HBV genomes is significantly reduced in Alix-deficient cells (Figure 5, H–I). Western blot analysis using Alix- and HBcAg-specific antibodies revealed that in the case of the NT cells, Alix and HBcAg are present in fractions 6 and 7 (Figure 5, J). In the KO cells, the Alix-specifc signal was undetectable, and HBcAg was not detectable in the exosomal fractions (fractions 6, 7) (Figure 5, J). However, rescue of the Alix-deficient cells by overexpression of mCherry-hAlix restored the exosomal release of HBV from these cells as evidenced by qPCR (Figure 5, H–I) and by HBcAg-specific Western blot analysis (Figure 5, J). The rescue was proven by detection of mCherry-hAlix protein in the exosomal fraction of the gradient (Figure 5, J). Additionally, overexpression of Alix seemed to change the characteristics of exosomes as the exosomal HBV fractions slightly shifted to a lower density. The excessive exosome secretion from Alix overexpressing cells could also potentially contribute to its altered distribution in the density gradient as compared with NT cells (Figure 5, H–I).

Figure 3. (See previous page). Separation of free HBV virions and naked capsids from exosomal HBV. A, Gradient purified free HBV virions (see schematic representation in Figure 2, C) with or without prior treatment with 0.5 % NP-40 for 40 minutes at 37 °C were being subjected to iodixanol gradient re-centrifugation. Copy number of HBV genomes in gradient fractions was quantified by qPCR. The *black line* shows the distribution of the untreated input; the *red line* is the NP-40 treated input. The density is shown by the *gray line*. B, Gradient purified free HBV virions treatment with 0.5 % NP-40 for 40 minutes at 37 °C (*red line*) or without prior treatment with NP-40 (*black line*) were being subjected to sucrose density gradient centrifugation. Copy number of HBV genomes in gradient fractions was quantified by qPCR. The density is shown by the *gray line*. C, Quantification of core antigen by ELISA in fraction 12 (NP-40-untreated) and fraction 15 (NP-40-treated) of the sucrose gradient (Figure 3, B) without and with Triton X-100 pretreatment. Unpaired parametric *t* tests for all panels; ***$P < .001$. D, Sucrose density gradient of iodixanol gradient purified exosomes after pretreatment without (*black line*) or with 0.25 % NP-40 (*red line*) for 20 minutes at 30 °C. Copy number of HBV genomes in gradient fractions was quantified by qPCR. The density is shown by the *gray line*. E, HBV virions were visualized by phosphotungstic acid negative staining of fractions 11 and 12 (NP-40-treated) of the sucrose gradient in Figure 3D. The *arrows* highlight the virus. F, Western blot analysis of the fractions of the sucrose gradient centrifugation of the untreated input and of the NP-40-treated input shown in Figure 3, D. For detection, the LHBs- and core-specific antibodies and the Alix-specific antibody were instrumental. G, Quantification of core antigen by HBcAg-specific ELISA in fractions 8, 11, 12, and 14, 15 of the sucrose gradients (Figure 3, D) without and with Triton X-100 pretreatment. Unpaired parametric *t* tests for all panels; *$P < .05$; ***$P < .001$. H, Sucrose density gradient of iodixanol gradient purified exosomes after pretreatment without (*black line*) or with 0.5 % NP-40 (*red line*) for 1 hour at 37 °C. Copy number of HBV genomes in gradient fractions was quantified by qPCR and shown in the upper panel. The density is shown by the *gray line*. The HBcAg distribution over the gradient of 0.5 % NP-40-treated input was analyzed by Western blot and shown in the *lower panel*. I, Phosphotungstic acid stain followed by TEM imaging of naked capsids detected in fractions 14, 15 (NP-40-treated) of the sucrose gradient shown in Figure 3, H or detected in fraction 15 (NP-40-treated) of the sucrose gradient shown in Figure 3, D. *Arrows* highlight the naked capsids.

Moreover, the impact of Syntenin KO on the release of exosomal HBV was studied. Syntenin interacts with Alix via LYPXnL motifs and plays a role for generation of intraluminal vesicles, which constitute a major source of exosomes.[38] Stable Syntenin KO cell lines based on HepAD38 cells were established by CRISPR/Cas9 system.
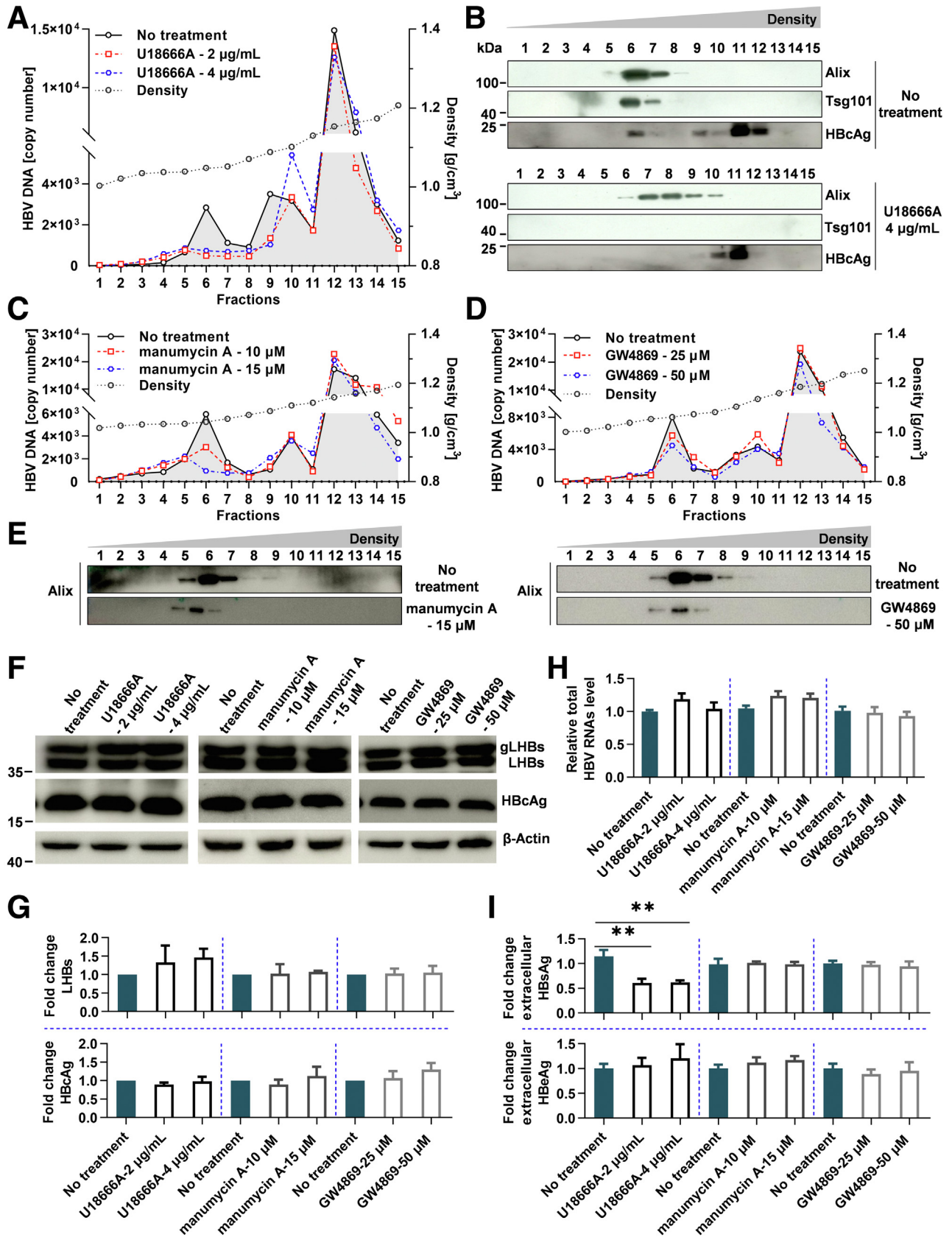
Endogenous Syntenin was effectively eliminated in HepAD38 KO cells as evidenced by Western blotting (Figure 5, B). Detection of HBV replication and HBsAg production in the Syntenin-deficient HepAD38 cell lines showed comparable levels of the intracellular HBcAg (Figure 5, C), intracellular HBV total RNA levels (Figure 5, D), HBV genomic DNA in the supernatants (Figure 5, E), extracellular HBsAg (Figure 5, F), and extracellular HBeAg (Figure 5, G) as compared with NT cells. Also, similar to knockout of Alix, a lower amount of N-glycosylated species of LHBs was detected in Syntenin-knockout HepAD38 cell lines (Figure 5, C). Likewise, analysis of the fractions from iodixanol gradient centrifugation by qPCR revealed that in the exosomal fractions (fractions 6 and 7) derived from the Syntenin KO cells the amount of HBV genomes is reduced as compared with the exosomal fractions of the control (NT) cells (Figure 5, K–L).

These data indicate that inhibition of exosome formation/release prevents the release of membrane wrapped HBV-particles.

Visualization of HBV Particles Within Exosomes by Electron Microscopy

The most widely used method for visualizing exosomes is negative staining and subsequent analysis by TEM.[39] However, this approach is not sufficient to study the internal structures of exosomes because the negative staining is limited to the surface and does not penetrate the lipid membrane.[40] Therefore, ultra-thin sections of fixed exosomes were analyzed to observe the presence of HBV virions within exosomes. TEM of Epon-embedded sections and methylcellulose/uranyl acetate stained cryo-sections demonstrated that viral particles with a diameter around 45 nm were frequently detected within exosomal structures (Figure 6, A). Moreover, in cryo-sections, the dense viral envelope surrounding the nucleocapid could be detected at membrane-cloaked viral structures (Figure 6, A, asterisk). To corroborate the observation that indeed intact HBV particles are found within exosomal structures, immunogold labeling of the cryo-sections was performed using either an anti-CD63 antibody or an antiserum against the preS1/preS2 domain (K112-4). Specific labeling for CD63 was localized to the surface of these sectioned vesicles (Figure 6, B). The LHBs-specific labeling was found within the lumen of some exosomes, where sometimes clearly identifiable enclosed viruses were observed (Figure 6, C, asterisk). Moreover, there was a LHBs-specific staining detectable on the surface of exosomes as further evidenced in Figure 6, C (orange arrows).

Taken together, the electron microscopy analysis supports the conclusion that exosomes derived from HBV-producing cells harbor intact HBV virions.

Infectivity and Neutralization of HBV-hijacked Exosomes

To investigate whether the exosomal HBV particles are infectious, the exosomal fractions (fractions 8 and 10) from the iodixanol gradient for control of the fractions representing free virions (fractions 13, 14) were prepared and used for infection of HepG2 cells or susceptible differentiated HepaRG cells (dHepaRG) (Figure 7, A). Instead of an identical multiplicity of infection, the same volume of each fraction of the same density gradient was used. This was done to control the potential impact of contaminations by free virions, which should be higher in the later exosomal fractions.

Neither the exosomal fraction (fraction 8) nor the virus fraction (fraction 13) was able to infect HepG2 cells (Figure 7, B).

However, in case of differentiated HepaRG cells, a productive infection by the exosomal fraction (fraction 8) pre-incubated with a control antibody (anti-His) could be observed. The infection was blocked by the receptor-binding domain (RBD)-specific antibody MA18/7 (Figure 7, C).

In contrast to the pure exosomal fraction, the later fraction 10, which is closer to the free viral fraction, initiated no productive infection (Figure 7, C). This suggests that infections established by the pure exosomal fraction were

Figure 4. (*See previous page*). **Inhibition of MVB- or exosome-formation impairs release of membrane-cloaked HBV virions.** *A*, HBV genome distributions in iodixanol density gradient of exosomes purified from the supernatant of HepAD38 cells. Cells were treated with 2 μg/mL (*red dotted line*) or 4 μg/mL U18666A (blue dotted line) for 48 hours or left untreated (*black line*). Viral genomes were quantified by qPCR. *B*, Western blot analysis of the fractions of the iodixanol gradient centrifugation (Figure 4, *A*) of the input derived from untreated cells (*upper panel*) or with U18666A-treated cells (*lower panel*). For detection, Alix- and Tsg101-specific antibodies- and core-specific antibodies were instrumental. *C*, HBV genome distributions in iodixanol density gradient of exosomes purified from the supernatant of HepAD38 cells treated with 10 μM (*red dotted line*) or 15 μM of manumycin A (*blue dotted line*) for 48 hours or untreated cells (*black line*). The viral genomes were quantified by qPCR. *D*, HBV genome distributions in iodixanol density gradient of exosomes purified from the supernatant of HepAD38 cells treated with 25 μM (*red dotted line*) or 50 μM GW4869 (*blue dotted line*) for 48 hours or untreated cells (*black line*). The viral genomes were quantified by qPCR. *E*, Alix distributions in an iodixanol-based density gradient (Figure 4, *C–D*) of exosomes purified from the supernatant of HepAD38 cells treated with manumycin A (*left panel*) or GW4869 (*right panel*) for 48 hours or untreated cells. *F*, Representative Western blot of the intracellular LHBs and HBcAg from HepAD38 cells treated with U18666A (*left panel*) or manumycin A (*middle panel*) or GW4869 (*right panel*) for 48 hours or from untreated cells. Detection of β-actin served as loading control. *G*, Quantification of intracellular LHBs (*upper panel*) and HBcAg (*lower panel*) signals in Figure 4, *F*. Fold change compared with untreated cells. Unpaired parametric *t* tests for all panels. *H*, HBV total RNAs expression levels from HepAD38 cells treated with U18666A or manumycin A or GW4869 for 48 hours or untreated cells. HBV total RNA were quantified by reverse transcription qPCR, and the relative expression levels to RPL27 mRNA were plotted as fold change to untreated cells. Unpaired parametric *t* tests for all panels. *I*, The extracellular levels of HBsAg (*upper panel*) and HBeAg (*lower panel*) in U18666A-, manumycin A-, or GW4869-treated HepAD38 cells were measured by ELISA. The fold change with untreated cells was plotted. Unpaired parametric *t* tests for all panels; **$P < .01$.

caused specifically by exosome-encapsulated viruses and argues against the possibility of a contamination by free viruses. In case of a contamination by free virus, more free viruses should be present in fraction 10.

Incubation with the purified virus (fraction 13/14) resulted in an effective infection as evidenced by onset of de novo HBsAg production after day 4. Preincubation with the RBD-binding MA18/7 impairs the infection (Figure 7, D).
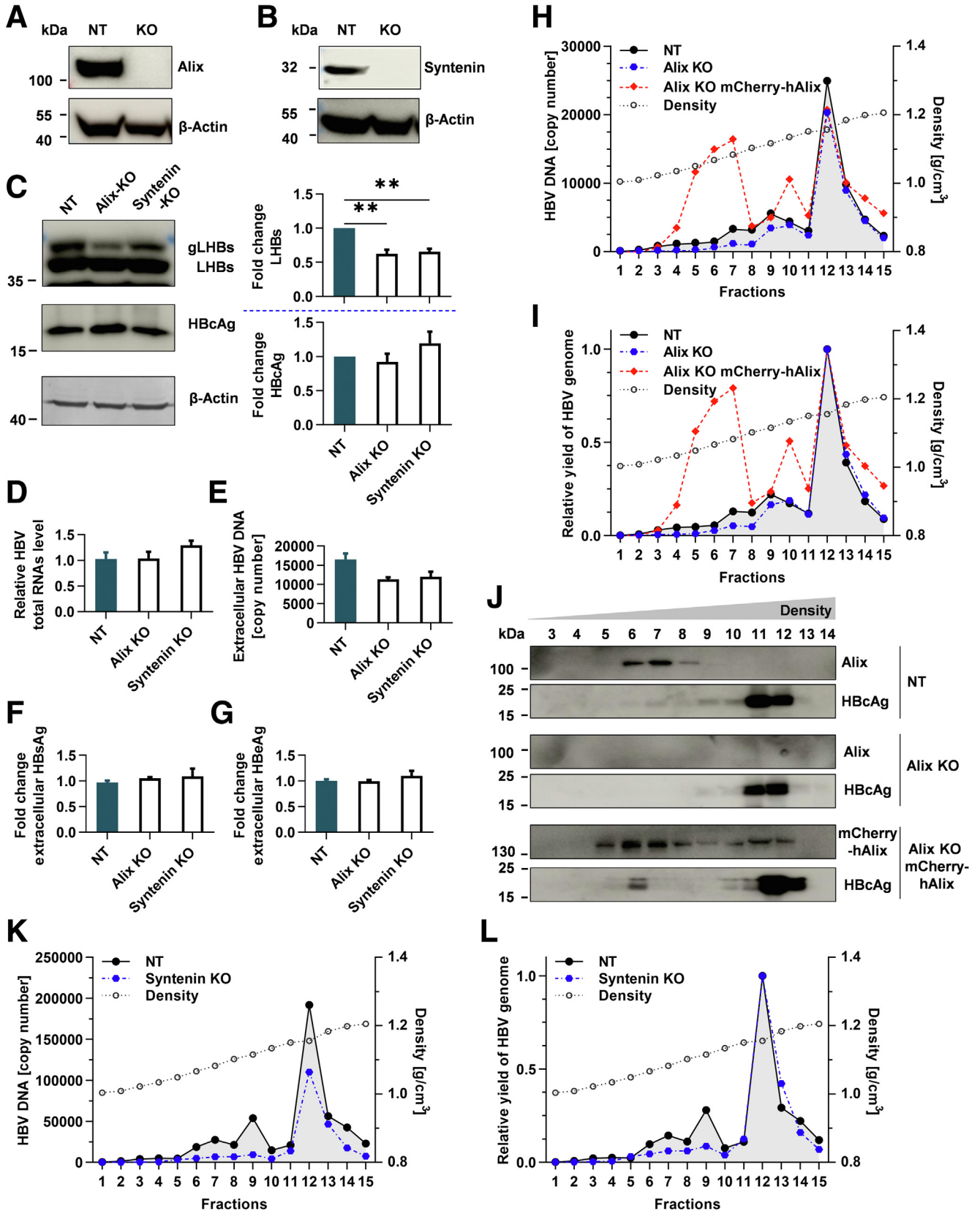
With respect to the HBsAg release there is a striking difference between cells infected with the exosomal fraction and the free virus. In the case of the exosomal infection, there is no continuous decrease of the HBsAg input until day 4 as in the case of the viral fraction. There is an initial decrease of the HBsAg level, which is interrupted by a resurgence of HBsAg levels at day 4, which is followed by a decrease of HBsAg. Interestingly, the resurgence of HBsAg release at day 4 is affected by MA18/7, suggesting that this process is probably dependent on the LHBs RBD (Figure 7, E).

The infection of differentiated HepaRG cells by exosomal HBV suggests that the presence of LHBs on the exosomal membrane plays a role for the internalization of exosomes derived from HBV-producing cells. In this case, the exosome-wrapped HBV virus is able to enter the host cells in a sodium-taurocholate co-transporter polypeptide (NTCP)-dependent manner. To clarify the contribution of NTCP in the infection established by exosome-encapsulated viruses in differentiated HepaRG cells, Myrcludex B, a synthetic peptide derived from the HBV L-protein, was used to block NTCP-mediated infection. Efficient infection resulting from incubation with purified virus (fraction 13) was inhibited by Myrcludex B-mediated blocking of NTCP-dependent entry (Figure 7, F). At the same time, blocking of the NTCP-mediated entry compromised HBV infection by exosomes in differentiated HepaRG cells as shown by the reduction of de novo synthesized HBsAg as compared with the untreated group (Figure 7, G).

Next, to further confirm the potential existence of exosomes delivering their encapsulated HBV virions to non-susceptible cells via exosome-targeted cell surface interactions, an additional inoculation of a 2-fold amount of purified exosomes used before was attempted in HepG2 cells. The use of these amounts of exosomes was able to initiate infection in HepG2-NTCP cells, as demonstrated by immunofluorescence staining of HBsAg at day 7 after inoculation (Figure 8, A). Interestingly, HBsAg-positive cells in very limited numbers were also be found in HepG2 cells inoculated under the same conditions (Figure 8, B). The de novo synthetis of HBeAg could be detected in inoculated HepG2-NTCP cells, indicating the presence of an effective infection there as well (Figure 8, C). In inoculated HepG2 cells, HBeAg levels marginally above the cutoff value for HBeAg were detected (Figure 8, C). It reflects that the uptake of exosome encapsulated HBV takes place, but in a very inefficient way. The difference observed between these 2 cell lines with respect to the infection by HBV corroborates the observation that LHBs present on the surface of exosomes could mediate the uptake of these exosomes in HBV-susceptible cells.

Taken together, these data indicate that the exosomal fraction can initiate infection of differentiated HepaRG cells and HepG2-NTCP cells. This infection of permissive cells can be blocked both by the RBD-specific MA18/7 and by the entry inhibitor Myrcludex B. This could reflect that the LHBs found on the surface of exosomes is involved in the attachment/entry process in a LHBs/NTCP-dependent manner, or that after exosomal attachment to the cell surface virions are released and then entry is mediated via the receptor complex. In any case, the targeting of these HBV-carrying LHBs-decorated exosomes appears to be influenced as the same input shows a significant lower infectivity in HBV non-permissive HepG2 cells. Nevertheless, uptake of exosome-encapsulated HBV into non-susceptible HepG2 cells via exosome/cell surface interactions is possible, albeit with much lower efficiency.

Discussion

Recent studies have described that viruses can hijack exosomes for their release. Previous findings also reported that in exosomes derived from HBV-infected hepatocytes HBV components, including HBV DNA, RNA, and HBV proteins are detectable.[41,42] Our work then demonstrated and visualized for the first time that complete infectious HBV

Figure 5. (*See previous page*). **CRISPR/Cas9 mediated knockout of Alix or Syntenin in HepAD38 cells impairs the release of exosomal HBV virions.** *A–B*, Western blot analysis of cellular lysates derived from Alix-deficient HepAD38 cells (*A*) or Syntenin-deficient HepAD38 cells (*B*). Detection of β-actin served as loading control. *C*, Intracellular amount of LHBs and HBcAg from Alix- or Syntenin-deficient HepAD38 cells. Representative Western blots for LHBs, HBcAg, and β-actin are shown in the *left panel*. Quantification of LHBs and HBcAg signals are shown in the *right panel*; fold change compared with NT cells. Unpaired parametric *t* tests for all panels; **$P < .01$. *D*, HBV total RNAs expression levels from Alix- or Syntenin-deficient HepAD38 cells. HBV total RNA were quantified by reverse transcription qPCR, and the relative expression levels to RPL27 mRNA were plotted as fold change to NT cells. Unpaired parametric *t* tests for all panels. *E*, The amount of extracellular HBV DNA from NT cells or Alix- or Syntenin-deficient HepAD38 cells was evaluated by qPCR. Unpaired parametric *t* tests for all panels. *F–G*, Extracellular HBsAg levels (*F*) and extracellular HBeAg levels (*G*) in Alix- or Syntenin-deficient HepAD38 cells were measured by ELISA. Fold change compared with NT cells were plotted. Unpaired parametric *t* tests for all panels. *H–I*, HBV genome distributions in iodixanol density gradient of exosomes purified from the supernatant of HepAD38 NT cells (*black line*), of Alix-deficient HepAD38 cells (*blue dotted line*), and of Alix-deficient HepAD38 cells rescued by overexpression of mCherry-Alix (*red dotted line*). The viral genomes were quantified by qPCR. The absolute quantification was displayed in Figure 5, *H*. Fold change of each gradient to fraction 12 was shown in Figure 5, *I*. *J*, Western blot analysis of the fractions of the iodixanol gradient centrifugation (Figure 5, *H–I*) of the input derived from HepAD38 NT cells (*upper panel*) or from Alix-deficient HepAD38 cells (*middle panel*) or from Alix-deficient HepAD38 cells rescued by overexpression of mCherry-hAlix (*lower panel*). For detection, the Alix-specific and the core-specific antibodies were instrumental. *K–L*, HBV genome distributions in iodixanol density gradient of exosomes purified from the supernatant of HepAD38 NT cells (*black line*) or of Syntenin-deficient HepAD38 cells (*blue dotted line*). The viral genomes were quantified by qPCR. The absolute quantification is displayed in Figure 5, *K*. Fold change of each gradient to fraction 12 is shown in Figure 5, *L*.
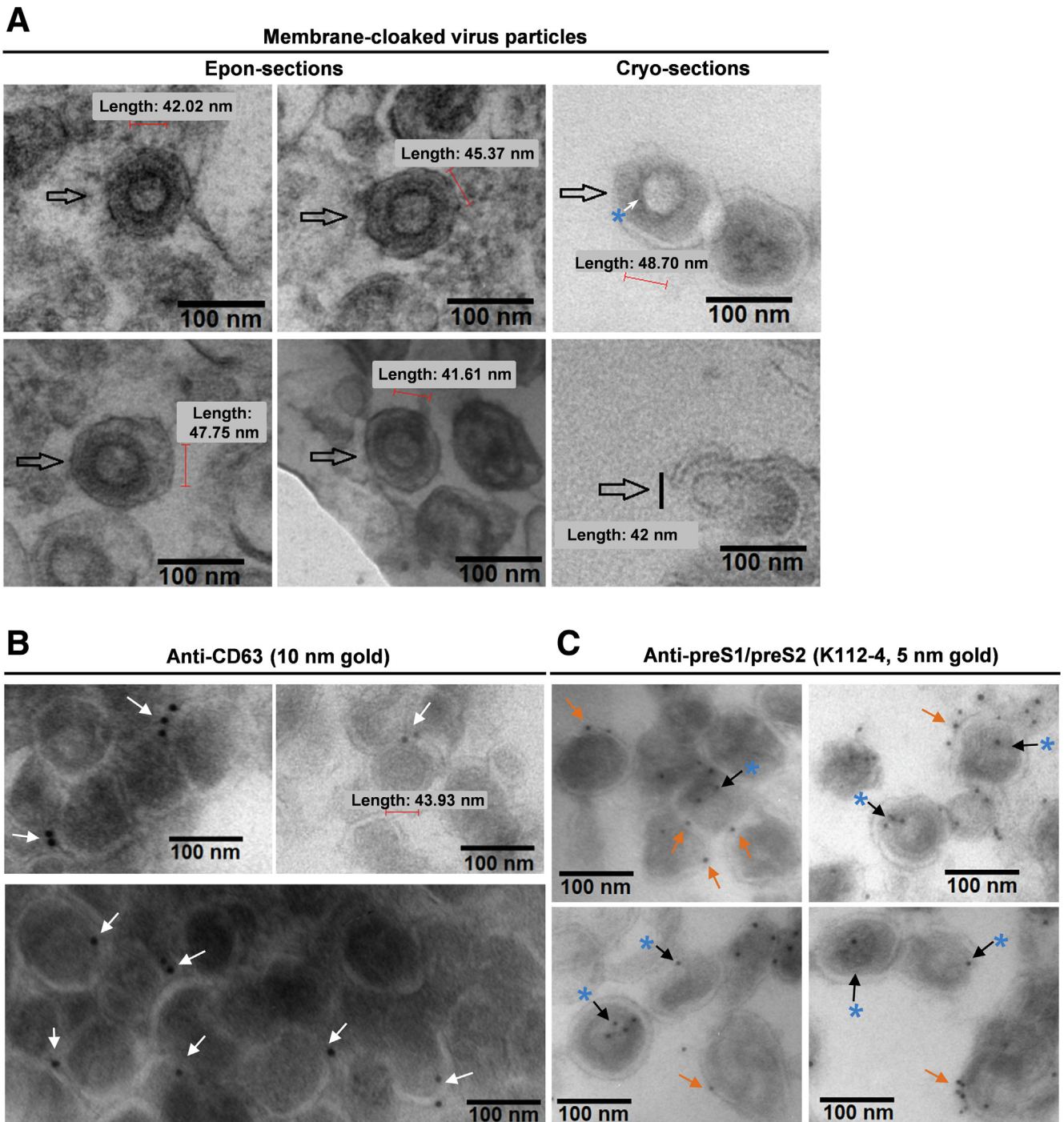
A

Membrane-cloaked virus particles

Epon-sections

Length: 42.02 nm

Length: 45.37 nm

Cryo-sections

Length: 48.70 nm

100 nm

100 nm

100 nm

Length: 47.75 nm

Length: 41.61 nm

100 nm

100 nm

Length: 42 nm

100 nm

B

Anti-CD63 (10 nm gold)

Length: 43.93 nm

100 nm

100 nm

100 nm

C

Anti-preS1/preS2 (K112-4, 5 nm gold)

100 nm

100 nm

100 nm

100 nm

Figure 6. Transmission electron microscopy of exosomes released from HepAD38 cells. *A*, TEM images from ultra-thin sections of Epon-embedded (*left*) or cryo-sections (*right*) of fixed exosomes showing virions enclosed by a membrane structure (*labeled by arrows*). An *asterisk* indicates that a dense viral envelope stands out from the surrounded nucleocapsid. *B–C*, Immunogold labeling of ultra-thin thawed cryo-sections of fixed exosomes. The cryo-sections were either labeled with an anti-CD63 antibody (visualized by 10-nm gold particles) or an anti LHBs antiserum (anti-preS1/preS2 domain rabbit serum [K112-4]) (visualized by 5-nm gold particles). *Arrows* indicate specific colloidal gold labeling. *Asterisks* represent that anti-LHBs (5 nm) is located at identifiable enclosed virus like particles. The surface of cryo-sectioned exosomes was also labeled by anti-LHBs (*orange arrows*).

particles can be found in exosomes. The presence of LHBs on the surface of these exosomes provides them the ability to attenuate the effect of antibodies to neutralize HBV virus and could be relevant for the interaction with target cells.

Like the previous detection of quasi-enveloped HAV and hepatitis E viruses, the discovery of these host membrane-cloaked HBV blurs the classic definition of HBV-enveloped particles and might change the conventional understanding

on the life cycle of HBV.[43] We describe here that the cell culture supernatant of HBV-expressing hepatoma cells contains 2 infectious populations with distinctly different buoyant density. Limited detergent treatment of the fraction with lower density caused successive release of the Dane particles, which can be further processed to naked capsids. These methods have also been successfully used for identifying other host membrane-wrapped viruses,[26] cargo types,[44] and for analysis of the membrane stability of exosomes.[45] The presence of intact virions within exosomes was further confirmed by electron microscopy. Ultrathin sectioning is a powerful method for observation of the inner lumenal structure of exosomes.[46-48] Immuno-gold labeling of the ultrathin sections directly showed the presence of HBV in exosomal structures.

To further delineate release pathway for membrane-wrapped HBV, 3 different inhibitors of exosome release were used, and all of them impaired the exosomal release of HBV. This was further corroborated by the establishment of Alix- or Syntenin-deficient cells. Gain and loss of function studies clearly underline the relevance of Syntenin-Alix for the formation of intraluminal vesicles[49-51] and exosomal release of HBV. Depletion of Syntenin reduces exosome turnover, indicating a definite impact on the amount of loaded cargo.[52] Therefore, it cannot be concluded that Syntenin is directly involved in sorting HBV into exosomes. However, the drastically increased release of exosomal HBV after rescue of Alix-deficient cells by overexpression of mCherry-Alix fusion construct, while the release of free HBV virions is not affected, underlines the relevance of Alix for the release of exosomal HBV. Consistent with the earlier study, our knockout and rescuing data added further evidence that Alix is dispensable for the release of free HBV virions.[4] Inhibition of the exosomal release does not lead to a significant change in the number of released free viral particles. This suggests that there is no significant flow between these 2 pathways or that there is no further capacity for release of free virions. Moreover, these data argue against the possibility that a fraction of free virions is formed by disassembly of exosomes. If this is the case, a decrease in exosomal release would be associated with a decrease of free virions. However, strictly spoken, it cannot be excluded that a decrease of exosome-derived free virions is compensated by an elevated release of free virions.

The other 2 interesting exosomal proteins, CD63 and TSG101, were shown to be involved, respectively, in the incorporation of LHBs in HBV envelope[53] and in the release of HBV by interacting with α-taxilin.[54] These functions might also contribute to the process of exosomal HBV virus formation due to the fact that they were both shown to be essential for the biogenesis of MVBs/exosomes.[38,55] Therefore, it would be interesting to explore their functions in further details. Also as shown in this study, because membrane-encapsulated virus is not the predominant mode of HBV release, the formation of exosome-encapsulated HBV cannot be excluded as an incidental possibility of long-term crosstalk between the virus and the host cells. If host factors are involved in the

hitchhiking of HBV on exosomes, it remains an interesting but unknown challenge under which conditions the exosomal membrane-encapsulated virus is triggered and under which conditions it is released as free virus via the MVB platform.

Consistent with a potential function of classical HBsAg spheres and filaments in HBV to deviate the immune response,[56] the presence of LHBs in the membrane of exosomes could confer them a similar function. This would require that before opsonization the virus can escape from the antibody decorated exosomes or it could be an (inefficient) strategy to enable infection of non-hepatic tissues as described in some reports.[57-60] In addition to wrapping viral factors, a large number of host proteins involved in various biological processes have been observed in exosomes released from hepatocytes as well. This reflects that they have many other roles besides our main focus on the ability of exosomes to transport viruses. A proteomics-based analysis showed that a certain number of proteasome subunit proteins were loaded in HepAD38-derived exosomes. It was speculated that this could give these exosomes the potential to mediate trans-cellular immune regulation.[42]

Another function which is ascribed to subviral particles in HBV infection is their enhancement of viral infection.[61] Exosomes derived from HBV-positive cells appear to have the same function; the enhancement could be exerted by the LHBs on surface of exosomes. Moreover, apart from the virion, the cargo of the exosome could affect the infection process. The infection of differentiated HepaRG cells could be blocked by the LHBs-specific neutralizing monoclonal MA18/7 and by cell entry inhibitor Myrcludex B. Various modes of actions can be discussed; the hepatocyte-exosome-interaction mediated by LHBs on the exosome surface is blocked, and this prevents binding of the exosome and its subsequent internalization. A further possibility is that the exosome disassembles in close vicinity to the membrane of the target cell, the virus is released, and the released virus is blocked by the neutralizing monoclonal MA18/7; the presence of Myrcludex B can also block the entry of the released virus. These hypotheses are consistent with the well-established tissue specificity of HBV. We failed to productively infect non permissive HepG2 cells by the same input of exosomal HBV used in HBV-susceptible cells. This could be due to the relative low number of exosomes used for infection or the fact that HBV as a cargo affects the target specificity of exosomes. But increasing the amount of input verified to the point that uptake of exosome-encapsulated HBV into non-permissive HepG2 cells is still possible. This very low uptake efficiency of exosomal HBV in non-susceptible cells could be causative for the rare event of detection of HBV (infection) in non-hepatic tissues.[57-60]

In conclusion, our findings reveal the existence of intact HBV virions present in exosomes. These exosomes carrying membrane-wrapped HBV particles can spread productive infection to differentiated HepaRG cells and HepG2-NTCP cells. This previously undiscovered strategy

of sequestering HBV particles in exosomes could be a strategy to escape from the immune response and to target them protected by the exosomal membrane to the hepatocyte. Exosomes that carry HBV particles seem also to have the potential to deliver HBV to non-permissive cells with low efficiency. This suggests that exosomes
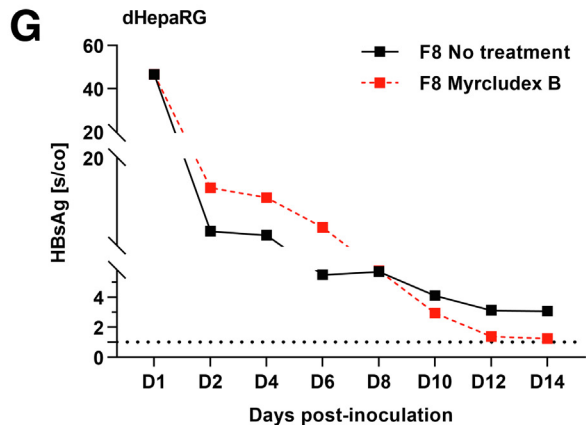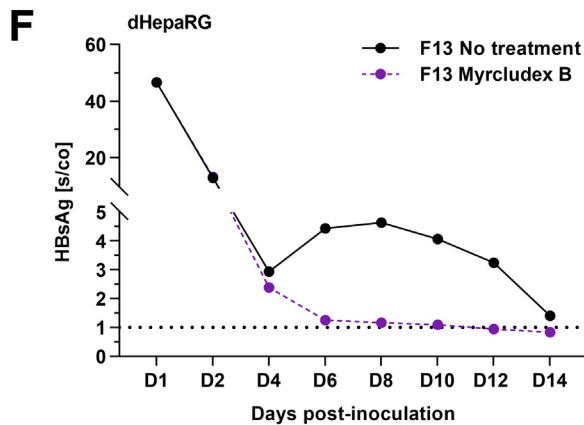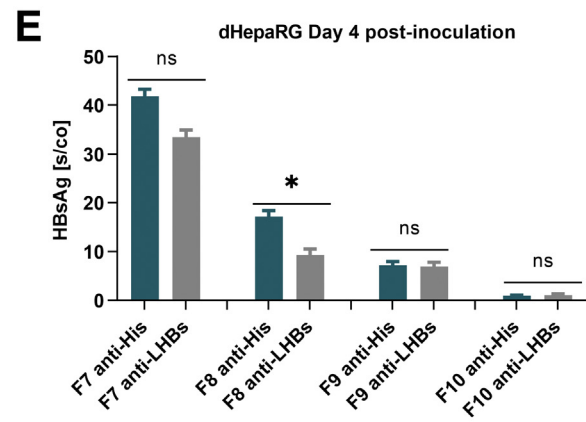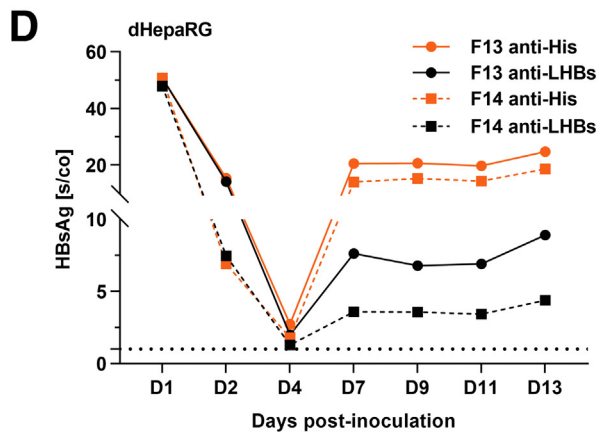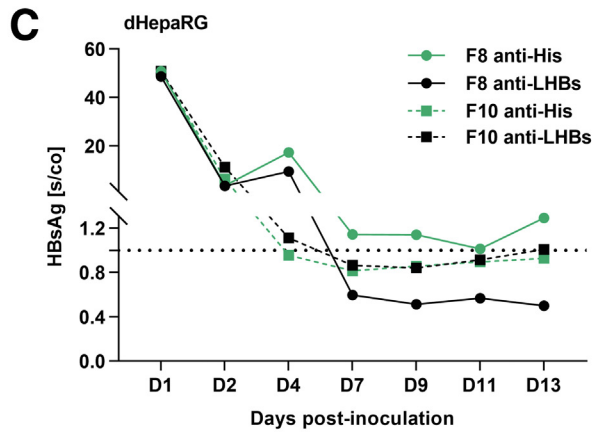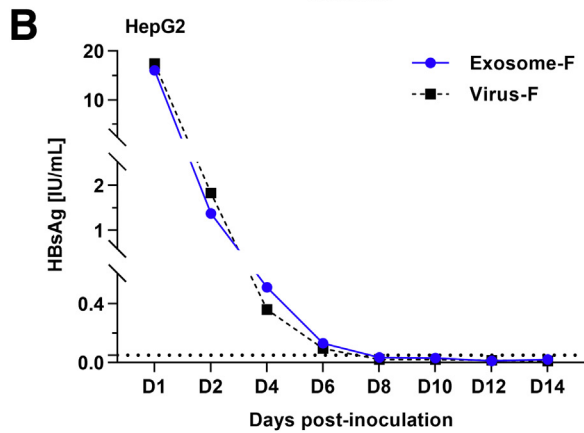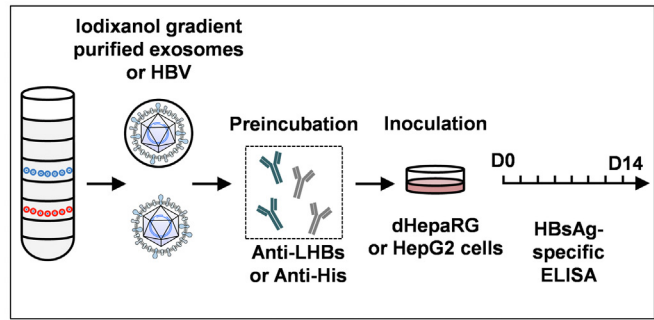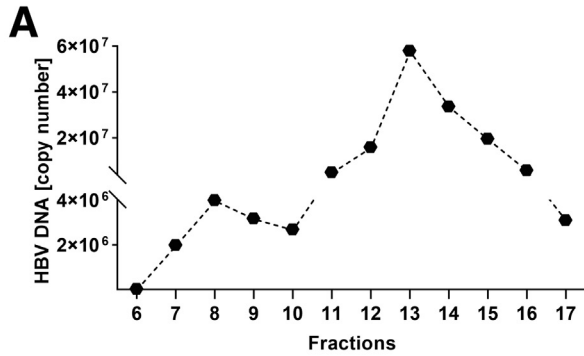
could be an additional factor that contributes to the spread of HBV.

Material and Methods
Cell Culture

HepG2 and Huh7 cells were maintained in Roswell Park Memorial Institute Medium-1640 and Dulbecco's Modified Eagle Medium supplemented with 10% (v/v) fetal bovine serum (FBS) (FBS.S 0615, Bio & Sell GmbH), 2 mM L-glutamine (Q), 100 μg/mL streptomycin (S), and 100 U/mL penicillin (P), respectively. HepAD38 cells[62] were grown in Dulbecco's Modified Eagle Medium supplemented with 10% (v/v) FBS, 2 mM Q, 100 μg/mL S, 100 U/mL P, and with 50 μM hydrocortisone 21-hemisuccinate (sc-250130, Santa Cruz) and 5 μg/mL insulin (I6634-100MG, Sigma-Aldrich) in addition. Cultivation and differentiation of HepaRG cells were performed as described[63]; the HepaRG cells were first maintained in William's E growth medium supplemented with 10% (v/v) FBS, 100 μg/mL S, 100 U/mL P, 5 μg/mL insulin, and 50 μM hydrocortisone 21-hemisuccinate for 2 weeks. Then, they were maintained in differentiation medium, growth medium added with 2% (v/v) dimethyl sulfoxide (M6323.0250, Genaxxon), for 2 more weeks. The medium was changed every 2 to 3 days. After 28 days, the HepaRG cells were used for infection.

Exosome Isolation

Exosomes from the cell culture supernatant were enriched based on differential ultracentrifugation according to a previously described method[39] with modifications. Samples of 35 mL of cell culture supernatant were centrifuged at 10,000 $\times$ g for 40 minutes with rotor SW 32 (369650, Beckman) to remove cell fragments and other debris. The supernatant was then ultracentrifuged at 100,000 $\times$ g for 70 minutes to isolate the exosomes. The pellet was resuspended in 1 mL phosphate buffered saline (PBS) and was placed onto a discontinuous density gradient. To prepare the discontinuous gradient, 50%, 40%, 30%, 20%, and 10% (w/v) iodixanol or sucrose solutions were made by diluting a stock solution of 60% (w/v) iodixanol (OptiPrep, 1114542, ProgenBiotechnik) or 60% (w/v) sucrose/PBS (4621.2, Carl Roth) with PBS (pH 7.1). Aliquots (1.5 mL) of 60 % to 10 % (w/v) iodixanol or sucrose solution were sequentially layered in a polypropylene ultracentrifuge tube (331372, Beckman), and 1 mL resuspended exosomes was carefully overlaid onto the top of the gradient. Centrifugation was carried out at 125,000 $\times$ g for at least 18 hours with SW 41 rotor (331336, Beckman) for further purification. After centrifugation, gradients were fractionated in 0.5 mL fractions from the top. The refractive index of each fraction was measured by Refractometer (Bausch & Lomb, Laval, Canada). All centrifugation steps were performed at 4 °C by Optima XPN-80 Ultracentrifuge (Beckman Coulter, Brea, CA).

Western Blot Analysis and Antibodies

Samples were denatured in sample loading buffer at 100 °C for 10 minutes and separated by sodium dodecyl-sulfate polyacrylamide gel electrophoresis. The proteins were transferred onto a polyvinylidene difluoride membrane (P667.1, Carl Roth). For detection of the blotted proteins the following primary antibodies were used: anti-Alix MAb (sc-271975, SantaCruz), anti-Tsg101 MAb (sc-7964, SantaCruz), anti-CD63 Mab (ab59479, Abcam), anti-LHBs MAb (MA18/7,[64] kindly provided by Dr. Glebe Giessen), anti-HBcAg polyclonal antibody (K46, a gift from Reinhild Prange, Department of Medical Microbiology and Hygiene, Johannes Gutenberg-Universität Mainz, Mainz, Germany), or rabbit anti-syntenin antibody (22399-1-AP, Proteintech Europe). Secondary antibodies used were Amershan ECL horseradish peroxidase-linked sheep anti-mouse IgG (NA931-1ML, GE Healthcare) and donkey anti-rabbit IgG (NA934-1ML, GE Healthcare). Bound antibodies were visualized by enhanced chemiluminescence reagent Immobilon Western Chemiluminescent HRP Substrate (WBKLS0100, Merck Millipore, Darmstadt, Germany), using an ImageQuant800 system

Figure 7. (*See previous page*). **Inoculation of HepG2- and differentiated HepaRG cells by exosomal HBV and free HBV.** *A*, HBV genome copy number in each exosomal and viral inoculum is shown in the *left*. Schematic description of the infection experiment procedure is shown in the *right*. *B*, HBsAg ELISA of supernatant derived from HepG2 cells inoculated either with exosomal HBV virions or free HBV virions. Medium was changed at the indicated time points and analyzed by HBsAg ELISA. The *horizontal dotted line* indicated the cutoff value. *C*, HBsAg ELISA of supernatant derived from differentiated HepaRG cells inoculated either with exosomal HBV (fraction 8 of the iodixanol gradient) or a less pure, later exosomal fraction (fraction 10). The inoculum was preincubated with the LHBs-specific antibody MA18/7 (1 μg/mL) or an anti-hexa-His-specific monoclonal antibody (1 μg/mL) as control. Medium was changed at the indicated time points and analyzed by HBsAg-specific ELISA. S/CO, Sample to cutoff signal. The cutoff value is represented by the *horizontal dotted line*. *D*, HBsAg ELISA of supernatant derived from differentiated HepaRG cells inoculated with free HBV virions (fractions 13 and 14). The inoculum was preincubated with the LHBs-specific antibody MA18/7 (1 μg/mL) or an anti-hexa-His-specific monoclonal (1 μg/mL) as control. Medium was changed at the indicated time points and analyzed by HBsAg-specific ELISA. The *horizontal dotted line* delineates the cutoff value. *E*, HBsAg ELISA of supernatant derived from differentiated HepaRG cells inoculated either with exosomal HBV (fractions 7, 8 of the iodixanol gradient) or a less pure, later exosomal fraction (fractions 9, 10 of the iodixanol gradient). The inoculum was preincubated with the LHBs-specific antibody MA18/7 (1 μg/mL) or an anti-hexa-His-specific monoclonal (1 μg/mL) as control. Here, the HBsAg content at day 4 of the different samples is analyzed. Unpaired parametric *t* tests for all panels; **$P < .01$; ***$P < .001$; ns, not significant. *F–G*, Differentiated HepaRG cells were inoculated with free HBV virions (fractions 13) (*F*) or exosomal HBV (fraction 8 of the iodixanol gradient) (*G*), and secreted HBsAg was quantified at the indicated time points by HBsAg-specific ELISA. Myrcludex B 500 nM was added during infection. The *horizontal dotted line* indicates the cutoff value.
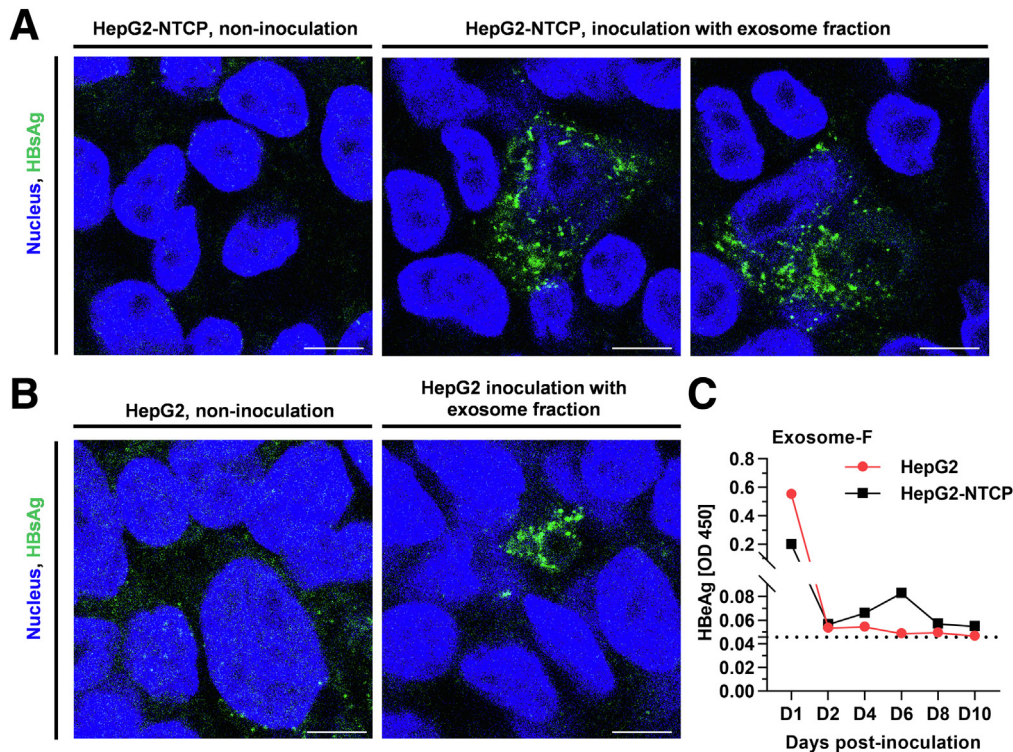
Figure 8. Inoculation of HepG2-NTCP and HepG2 cells by exosomal HBV isolated from the supernatant of HepAD38 cells. *A*, Representative immunofluorescence staining of HBsAg (*green*) on day 7 of HepG2-NTCP cells inoculated with or without 2-fold amounts of the purified exosomes used in Figure 7; nuclei in *blue*, scale bar = 15.1 μm. *B*, Representative immunofluorescence staining of HBsAg (*green*) on day 7 of HepG2 cells inoculated with or without 2-fold amounts of the purified exosomes used in Figure 7; nuclei in *blue*, scale bar = 15.1 μm. *C*, Two-fold amounts of the purified exosomes used in Figure 7 were inoculated with HepG2 and HepG2-NTCP cells, and HBeAg in the supernatant of these cells was quantified by HBeAg-specific ELISA at the indicated time points. The *horizontal dashed line* represents the cutoff value.

(Cytiva Europe GmbH, Freiburg, Germany). Band intensities were quantified with ImageQuant TL (Cytiva Europe GmbH, Freiburg, Germany).

Quantification of HBV DNA and RNA

HBV DNA of each fraction from density gradient and HBV total RNA were measured by qPCR, using the Maxima SYBR green qPCR kit (K0221, Thermo Fisher Scientific, Braunschweig, Germany) and a LightCycler 480 instrument (Roche, Basel, Switzerland). Primers targeted HBV S-domain (Forward: 5'-GCACCTGTATTCCCATCCCA-3'; Reverse: 5'-CGAACCACT-GAACAAATGGC-3') or 60S ribosomal protein L27 (RPL27) as a housekeeping gene (Forward: 5'-AAAGCTGTCATCGTGAA-GAAC -3'; Reverse: 5'-GCTGCTACTTTGCGGGGGTAG-3') were used. Absolute quantification was used to quantify HBV DNA levels. The expression levels of HBV total RNA, normalized to RPL27, was analyzed using the $\Delta\Delta$CT method.

For HBV total RNA quantification, total RNA was isolated from cells using the peqGold TriFast reagent (30-2010P, Peqlab Biotechnologie GmbH, Erlangen, Germany). Then, RQ1 RNase-free DNase treated total cellular RNA was used to transcribe into cDNA using a random hexamer primer and RevertAid H Minus reverse transcriptase (EP0451, Thermo Fisher Scientific, Waltham, MA). 10-fold dilutions of cDNA with ddH$_2$O supplemented with 0.1% w/v DEPC were available for qPCR.

Nanoparticle Tracking Analysis

NTA was performed to measure the size range of the exosomes using a NanoSight NS300 instrument (Malvern Panalytical, Malvern, United Kingdom). The concentrated exosome pellet from cell culture supernatant of HepAD38 cells or HepG2 cells was diluted in filtered PBS to an appropriate concentration, and quadruple 60-second videos were recorded according to the manufacturer's instructions. Data were analyzed using NTA 3.3 software (Malvern Panalytical, Malvern, United Kingdom) with a detection threshold of 5.

ELISAs

HBsAg levels were determined by an Enzygnost HBsAg 6.0 kit (OPFM07(Q), Siemens Healthcare GmbH, Erlangen, Germany) and supplementary reagents kit for Enzygnost/TMB (OUVP17, Siemens Healthcare GmbH, Erlangen, Germany) according to the manufacturer's protocol. For analysis of membrane wrapped HBsAg, gradient fractions were treated with RIPA buffer followed by ultrasound treatment. For quantification of HBcAg, the QuickTiter HBV Core Antigen ELISA Kit (VPK-150, Cell Biolabs, INC, San Diego, CA) was used for capturing the nucleocapsids as recommended by the manufacturer. To destroy the exosomal membrane or to remove the viral envelope, differential treatment with 0.25% or 0.5% (v/v) NP-40 (74385, Fluka) was performed

as indicated. The quantification of HBeAg was performed by an HBeAg ELISA kit (CSB-E13557h, CUSABIO, Houston, TX) or an ARCHITECT HBeAg kit (6C32-27, Abbott GmbH, Wiesbaden, Germany).

Exosome Isolation With Immuno-magnetic Beads

Exosomes were isolated from the supernatant of HepAD38 by differential centrifugation, followed by iodixanol density gradient centrifugation. Then the exosomal fractions from the iodixanol gradient were incubated with CD63-coated Dynabeads (10606D, invitrogen) or unrelated Dynabeads M-280 Sheep Anti–Rabbit IgG (11203D, invitrogen), and mixed at 4 °C for 18 to 22 hours. The following day, the Dynabeads bound exosomes were washed for at least 4 times by removing the supernatant and adding 500 μL of isolation buffer (PBS with 0.1% bovine serum albumin [BSA], filtered through a 0.2-μm filter). After that, the exosomes on the magnetic beads were ready for Western blot analysis.

Whole-mounted Exosomes or HBV Virions Immunogold Labeling and Phosphotungstic Acid Staining

Immunogold labeling of exosomal fractions and HBV virions fraction from the iodixanol gradient were prepared as described[39] with modifications. In brief, glow discharged carbon-coated formvar grids were incubated with the samples for 20 minutes at room temperature (RT). Then the procedure was performed by floating the grids sequentially on drops containing either the PBS/50 mM glycine (3908.2, Carl Roth) for 3 minutes, the PBS/5% (w/v) BSA (T844.4, Carl Roth) blocking buffer for 30 minutes, the specified diluted primary mouse anti-CD63 antibody (ab59479, Abcam), or an antiserum against the preS1/preS2 domain of LHBs (K112-4, from rabbit) for 1 to 3 hours at RT, and secondary goat anti-mouse IgG conjugated with 10-nm gold (EM.GMHL10, BBI Solutions) or goat anti-rabbit IgG conjugated with 10-nm gold (EM.GAR10, BBI Solutions) for 1 hour at RT. After labeling, the grids were floating on a drop of 1% glutaraldehyde for 5 minutes to stabilize the immunoreaction, then washed twice in double distilled water and followed by 10-second 1% phosphotungstic acid negative staining.

The HBV virion fractions and nucleocapsid fractions obtained by NP-40 treatment of purified exosomes (derived from HepAD38 cells) were concentrated by ultracentrifugation in a Beckman TLA 110 rotor at 42,000 rpm for 2.5 hours and resuspended in TNE buffer (10 mM Tris–HCl [pH 7.4], 1 mM EDTA, 150 mM NaCl). For negative staining, glow discharged carbon-coated formvar grids were incubated with the enriched samples for 20 minutes at RT. After 2 washing steps with double distilled water, grids were stained with 1% phosphotungstic acid in ddH$_2$O for 10 seconds at RT and air-dried. All the grids were examined using a Zeiss EM-109 transmission electron microscope.

Cell Viability Assays

HepAD38 cells in 96-well plate were incubated with culture medium containing serial dilutions of U18666A (1–10 μg/mL, U3633-5MG, Sigma-Aldrich), manumycin A (1–50

μM, 52665-74-4, Cayman Chemical), or GW4869 (1–50 μM, D1692, Sigma-Aldrich) at 37 °C. After 48 hours, the cell viability was monitored using a PrestoBlue Cell Viability Reagent (Invitrogen, Waltham, MA) and a Tecan Microplate Reader (Infinite M1000, Tecan, Männedorf, Switzerland).

Inhibitors Treatment in HepAD38 Cells

For inhibition of MVBs or exosome generation, HepAD38 cells were plated into T175 flasks for 24 hours and treated with either culture media containing dimethyl sulfoxide or indicated concentrations of specific inhibitors. After 48 hours of treatment, exosomes were isolated from the cell culture supernatant by differential ultracentrifugation and discontinuous iodixanol gradient centrifugation as described above.

Generation of Alix or Syntenin KO Clones in HepAD38 Cells

Single-guide RNAs (sgRNAs) targeting Alix or Syntenin were chosen from GenScript gRNA database and cloned into the pSpCas9(BB)-2A-Puro (pX459) V2.0 plasmid (62988, Addgene) to generate CRISPR/Cas9 systems. Two CRISPR constructs were designed to target human *Alix* gene (exon 8; guide sequence: 5′-CGGGGTAGATTTCACAAGTG-3′) and *Syntenin* gene (exon7; guide sequence: 5′-ACA-GAATGTCATTGGATTGA-3′),[65] respectively. HepAD38 cells were transfected with pX459 plasmids with the above gRNAs inserted using FuGENE HD Transfection Reagent (PRE2311, Promega, Madison, WI). Forty-eight hours post-transfection, cells were treated with medium containing puromycin (2.5 μg/mL, P9620, Sigma-Aldrich) for 2 weeks. Stable KO clones were isolated, amplified, and analyzed by immunoblotting. For Alix-rescues experiments, HepAD38 Alix KO cells (5 × 10^6 cells per 150-mm dish) were transiently transfected using linear polyethyleneimine (9002-98-6, Polysciences) with 20 μg of human full-length Alix expression vector (mCherry-hALIX, 21504, Addgene). Exosomes were isolated from the supernatant at 48 hours post-transfection as mentioned above.

Exosome Ultra-thin Section Preparation and Immunolabeling-TEM

Visible exosome pellets were fixed with 0.1 M PHEM buffer containing 4% (v/v) formaldehyde (FA) (4979.1, Carl Roth) plus 0.1% (v/v) glutaraldehyde (EM grade, 3778.1, Carl Roth) at RT for 30 minutes.[66,67] Pellets were stored in 4% (v/v) FA in 0.1 M PHEM until use. After washing, fixed pellets were gently mixed with 3% (w/v) agarose, followed by centrifuging to form a pellet and trimming to cubes. The cubes were washed with PBS and embedded in epoxy resin according to standard preparation protocols before being cut into ultra-thin sections of 70 nm thickness.[68,69] The Epon sections were then transferred to 300-mesh copper grids and stained with 0.2% (v/v) uranyl acetate.

For cryo-sectioning, mixtures of 3% (w/v) low gelling temperature agarose with fixed exosomes were infiltrated with 2.3 M sucrose, frozen in liquid nitrogen, and then processed for 100 nm cryo-sections.[66] Sections were picked

up on a drop of cold 2.3 M sucrose and transferred onto the formvar surface of nickel grids.[67]

The immunolabeling procedure of cryo-sections was performed by floating the grids sequentially on drops containing either the 1% (w/v) milk (T145.4, Carl Roth) blocking buffer, the specified diluted primary mouse anti-CD63 antibody (ab59479, Abcam), or an antiserum against the preS1/preS2 domain of LHBs (K112-4, from rabbit), and secondary goat anti-mouse IgG conjugated with 10-nm gold (EM.GMHL10, BBI Solutions) or goat anti-rabbit IgG conjugated with 5-nm gold (EM.GAR5, BBI Solutions) at RT. After labeling, the grids were washed in distilled water and contrasted in a thin layer of 2% (w/v) methylcellulose (M7027-100G, Sigma) with 0.4% (v/v) uranyl acetate on ice for 10 minutes and air-dried.[70] All samples were examined using a Zeiss EM-109 transmission electron microscope.

Inoculation and Neutralization Assays of HBV-hijacked Exosomes

Exosomes were isolated from 400 mL HepAD38 cell culture supernatant by differential ultracentrifugation and iodixanol gradient as described above. Purified HBV-loaded exosomes or free HBV virus fractions were used for infection. Instead of an identical multiplicity of infection, the same volume of the exosomal fractions was used to exclude that infection could be caused by a contamination of free HBV virions. To the purified HBV exosomal fractions or free HBV virus fractions, the RBD-binding anti-preS1 antibody (MA18/7, 1 μg/mL) or an unrelated monoclonal anti-hexa-His antibody (sc-8036, Santa Cruz) was added and kept at 37 °C for 2 hours. The mixtures were then inoculated with differentiated HepaRG cells for 20 hours at 37 °C. In addition, a mixture of purified HBV exosomal fraction or free HBV viral fraction together with or without 500 nM Myrcludex B was also incubated with differentiated HepaRG cells for 20 hours at 37 °C. In parallel, HepG2 cells, which are insusceptible for HBV infection, and the susceptible HepG2-NTCP cells were also inoculated with exosomes or free HBV at 37 °C for 20 hours. At the end of incubation, cells were washed 4 times with PBS and maintained in their respective culture media. Afterwards, medium was refreshed and collected every other day up to 14 days post inoculation. Infection was analyzed by determination of the HBsAg or HBeAg amount in the supernatant collected at the indicated time points. For HepG2 and HepG2-NTCP cells, the infection at day 7 after inoculation was also detected by immunofluorescence.

Immunofluorescence Microscopy

Cells inoculated with or without purified exosomes on day 7 were fixed with 4% (v/v) FA for 20 minutes at RT, followed by permeabilization with 0.5% (v/v) Triton X-100 (T9284, Sigma) for 10 minutes at RT, and after subsequent blocking with 1% (w/v) BSA for 30 minutes at RT; immunofluorescence staining was performed. HBsAg was detected by incubating with a polyclonal FITC conjugated rabbit anti-HBsAg (ab32914, Abcam) at RT for 1 hour. The nucleus was stained by 4′,6-Diamidin-2-phenylindole (D1306, Invitrogen). Stained and Mowiol-mounted cells were

visualized using a confocal laser scanning microscope Leica TCS SP8 System with a DMi8 microscope (Leica, Wetzlar, Germany) under a 100× magnification oil immersion objective (numerical aperture = 1.4). Image acquisitions and analysis were performed with the LAS X Control Software.

Statistical Analysis

Results are presented by at least 3 replicate experiments independently unless stated otherwise. The statistical significance between each of the 2 groups was tested by unpaired parametric t tests except as noted otherwise. All statistical analyses were performed in GraphPad Prism 9.2.0 (GraphPad Software, San Diego, CA).

References

1. Liang TJ. Hepatitis B: the virus and disease. Hepatology 2009;49(5 Suppl):S13–S21.
2. Glebe D, König A. Molecular virology of hepatitis B virus and targets for antiviral intervention. Intervirology 2014; 57:134–140.
3. Watanabe T, Sorensen EM, Naito A, Schott M, Kim S, Ahlquist P. Involvement of host cellular multivesicular body functions in hepatitis B virus budding. Proc Natl Acad Sci U S A 2007;104:10205–10210.
4. Bardens A, Döring T, Stieler J, Prange R. Alix regulates egress of hepatitis B virus naked capsid particles in an ESCRT-independent manner. Cell Microbiol 2011; 13:602–619.
5. Sun D, Nassal M. Stable HepG2- and Huh7-based human hepatoma cell lines for efficient regulated expression of infectious hepatitis B virus. J Hepatol 2006; 45:636–645.
6. Jiang B, Hildt E. Intracellular trafficking of HBV particles. Cells 2020;9:2023.
7. Trépo C, Chan HLY, Lok A. Hepatitis B virus infection. Lancet 2014;384:2053–2063.
8. World Health Organization. Progress report on HIV, viral hepatitis and sexually transmitted infections 2019: accountability for the global health sector strategies, 2016–2021. World Health Organization, 2019.
9. Wandera BO, Onyango DM, Musyoki SK. Hepatitis B virus genetic multiplicity and the associated HBV lamivudine resistance mutations in HBV/HIV co-infection in Western Kenya: a review article. Infect Genet Evol 2022; 98:105197.
10. Gerlich WH. Medical virology of hepatitis B: how it began and where we are now. Virol J 2013;10:239.
11. Lavanchy D. Viral hepatitis: global goals for vaccination. J Clin Virol 2012;55:296–302.
12. Kian Chua P, Lin M-H, Shih C. Potent inhibition of human Hepatitis B virus replication by a host factor Vps4. Virology 2006;354:1–6.
13. Lambert C, Döring T, Prange R. Hepatitis B virus maturation is sensitive to functional inhibition of ESCRT-III, Vps4, and gamma 2-adaptin. J Virol 2007;81:9050–9060.
14. Jiang B, Himmelsbach K, Ren H, Boller K, Hildt E. Subviral hepatitis B virus filaments, like infectious viral

particles, are released via multivesicular bodies. J Virol 2015;90:3330–3341.

15. Patient R, Hourioux C, Roingeard P. Morphogenesis of hepatitis B virus and its subviral envelope particles. Cell Microbiol 2009;11:1561–1570.

16. Patient R, Hourioux C, Sizaret P-Y, Trassard S, Sureau C, Roingeard P. Hepatitis B virus subviral envelope particle morphogenesis and intracellular trafficking. J Virol 2007;81:3842–3851.

17. Macovei A, Petrareanu C, Lazar C, Florian P, Branza-Nichita N. Regulation of hepatitis B virus infection by Rab5, Rab7, and the endolysosomal compartment. J Virol 2013;87:6415–6427.

18. Bartusch C, Döring T, Prange R. Rab33B controls hepatitis B virus assembly by regulating core membrane association and nucleocapsid processing. Viruses 2017; 9:157.

19. Li J, Liu Y, Wang Z, Liu K, Wang Y, Liu J, Ding H, Yuan Z. Subversion of cellular autophagy machinery by hepatitis B virus for viral envelopment. J Virol 2011;85:6319–6333.

20. Hessvik NP, Llorente A. Current knowledge on exosome biogenesis and release. Cell Mol Life Sci 2018; 75:193–208.

21. Altan-Bonnet N. Extracellular vesicles are the Trojan horses of viral infection. Curr Opin Microbiol 2016; 32:77–81.

22. Nolte-'t Hoen E, Cremer T, Gallo RC, Margolis LB. Extracellular vesicles and viruses: are they close relatives? Proc Natl Acad Sci U S A 2016;113:9155–9161.

23. Feng Z, Hensley L, McKnight KL, Hu F, Madden V, Ping L, Jeong S-H, Walker C, Lanford RE, Lemon SM. A pathogenic picornavirus acquires an envelope by hijacking cellular membranes. Nature 2013;496:367–371.

24. Takahashi M, Yamada K, Hoshino Y, Takahashi H, Ichiyama K, Tanaka T, Okamoto H. Monoclonal antibodies raised against the ORF3 protein of hepatitis E virus (HEV) can capture HEV particles in culture supernatant and serum but not those in feces. Arch Virol 2008; 153:1703–1713.

25. Takahashi M, Tanaka T, Takahashi H, Hoshino Y, Nagashima S, Jirintai Mizuo H, Yazaki Y, Takagi T, Azuma M, Kusano E, Isoda N, Sugano K, Okamoto H. Hepatitis E virus (HEV) strains in serum samples can replicate efficiently in cultured cells despite the coexistence of HEV antibodies: characterization of HEV virions in blood circulation. J Clin Microbiol 2010;48:1112–1125.

26. Nagashima S, Takahashi M, Kobayashi T, Nishizawa T, Nishiyama T, Primadharsini PP, Okamoto H. Characterization of the quasi-enveloped hepatitis E virus particles released by the cellular exosomal pathway. J Virol 2017; 91:e00822–17.

27. Ramakrishnaiah V, Thumann C, Fofana I, Habersetzer F, Pan Q, de Ruiter PE, Willemsen R, Demmers JAA, Stalin Raj V, Jenster G, Kwekkeboom J, Tilanus HW, Haagmans BL, Baumert TF, van der Laan, Luc JW. Exosome-mediated transmission of hepatitis C virus between human hepatoma Huh7.5 cells. Proc Natl Acad Sci U S A 2013;110:13109–13113.

28. Kadiu I, Narayanasamy P, Dash PK, Zhang W, Gendelman HE. Biochemical and biologic

29. characterization of exosomes and microvesicles as facilitators of HIV-1 infection in macrophages. J Immunol 2012;189:744–754.

29. Madison MN, Okeoma CM. Exosomes: implications in HIV-1 pathogenesis. Viruses 2015;7:4093–4118.

30. Amara A, Littman DR. After Hrs with HIV. J Cell Biol 2003; 162:371–375.

31. Cocozza F, Grisard E, Martin-Jaular L, Mathieu M, Théry C. SnapShot: extracellular vesicles. Cell 2020; 182:262–262.e1.

32. Li P, Kaslan M, Lee SH, Yao J, Gao Z. Progress in exosome isolation techniques. Theranostics 2017;7:789–804.

33. Cantin R, Diou J, Bélanger D, Tremblay AM, Gilbert C. Discrimination between exosomes and HIV-1: purification of both vesicles from cell-free supernatants. J Immunol Methods 2008;338:21–30.

34. Konadu KA, Huang MB, Roth W, Armstrong W, Powell M, Villinger F, Bond V. Isolation of exosomes from the plasma of HIV-1 positive individuals. J Vis Exp 2016; 107:53495.

35. Elgner F, Ren H, Medvedev R, Ploen D, Himmelsbach K, Boller K, Hildt E. The intracellular cholesterol transport inhibitor U18666A inhibits the exosome-dependent release of mature hepatitis C virus. J Virol 2016; 90:11181–11196.

36. Primadharsini PP, Nagashima S, Takahashi M, Kobayashi T, Nishiyama T, Nishizawa T, Yasuda J, Mulyanto, Okamoto H. Multivesicular body sorting and the exosomal pathway are required for the release of rat hepatitis E virus from infected cells. Virus Res 2020;278: 197868.

37. Fujii K, Hurley JH, Freed EO. Beyond Tsg101: the role of Alix in 'ESCRTing' HIV-1. Nat Rev Microbiol 2007; 5:912–916.

38. Baietti MF, Zhang Z, Mortier E, Melchior A, Degeest G, Geeraerts A, Ivarsson Y, Depoortere F, Coomans C, Vermeiren E, Zimmermann P, David G. Syndecan-syntenin-ALIX regulates the biogenesis of exosomes. Nat Cell Biol 2012;14:677–685.

39. Théry C, Amigorena S, Raposo G, Clayton A. Isolation and characterization of exosomes from cell culture supernatants and biological fluids. Curr Protoc Cell Biol 2006, Chapter 3:Unit 3.22.

40. Choi H, Mun JY. Structural analysis of exosomes using different types of electron microscopy. Appl Microscopy 2017;47:171–175.

41. Wang J, Cao D, Yang J. Exosomes in hepatitis B virus transmission and related immune response. Tohoku J Exp Med 2020;252:309–320.

42. Jia X, Chen J, Megger DA, Zhang X, Kozlowski M, Zhang L, Fang Z, Li J, Chu Q, Wu M, Li Y, Sitek B, Yuan Z. Label-free proteomic analysis of exosomes derived from inducible hepatitis B virus-replicating HepAD38 cell line. Mol Cell Proteomics 2017;16(4 Suppl 1):S144–S160.

43. Feng Z. Quasi-enveloped hepatitis virus assembly and release. Adv Virus Res 2020;108:315–336.

44. Gangalum RK, Atanasov IC, Zhou ZH, Bhat SP. AlphaB-crystallin is found in detergent-resistant membrane microdomains and is secreted via exosomes from

human retinal pigment epithelial cells. J Biol Chem 2011; 286:3261–3269.

45. Kumeda N, Ogawa Y, Akimoto Y, Kawakami H, Tsujimoto M, Yanoshita R. Characterization of membrane integrity and morphological stability of human salivary exosomes. Biol Pharm Bull 2017;40:1183–1191.

46. Jung MK, Mun JY. Sample preparation and imaging of exosomes by transmission electron microscopy. J Vis Exp 2018;131:56482.

47. Kim SB, Kim HR, Park MC, Cho S, Goughnour PC, Han D, Yoon I, Kim Y, Kang T, Song E, Kim P, Choi H, Mun JY, Song C, Lee S, Jung HS, Kim S. Caspase-8 controls the secretion of inflammatory lysyl-tRNA synthetase in exosomes from cancer cells. J Cell Biol 2017; 216:2201–2216.

48. Heijnen HF, Schiel AE, Fijnheer R, Geuze HJ, Sixma JJ. Activated platelets release two types of membrane vesicles: microvesicles by surface shedding and exosomes derived from exocytosis of multivesicular bodies and alpha-granules. Blood 1999;94:3791–3799.

49. Friand V, David G, Zimmermann P. Syntenin and syndecan in the biogenesis of exosomes. Biol Cell 2015; 107:331–341.

50. Ghossoub R, Lembo F, Rubio A, Gaillard CB, Bouchet J, Vitale N, Slavík J, Machala M, Zimmermann P. Syntenin-ALIX exosome biogenesis and budding into multivesicular bodies are controlled by ARF6 and PLD2. Nat Commun 2014;5:3477.

51. Mir B, Goettsch C. Extracellular vesicles as delivery vehicles of specific cellular cargo. Cells 2020;9:1601.

52. Kashyap R, Balzano M, Lechat B, Lambaerts K, Egea-Jimenez AL, Lembo F, Fares J, Meeussen S, Kügler S, Roebroek A, David G, Zimmermann P. Syntenin-knockout reduces exosome turnover and viral transduction. Sci Rep 2021;11:4083.

53. Ninomiya M, Inoue J, Krueger EW, Chen J, Cao H, Masamune A, McNiven MA. The exosome-associated tetraspanin CD63 contributes to the efficient assembly and infectivity of the hepatitis B virus. Hepatol Commun 2021;5:1238–1251.

54. Hoffmann J, Boehm C, Himmelsbach K, Donnerhak C, Roettger H, Weiss TS, Ploen D, Hildt E. Identification of α-taxilin as an essential factor for the life cycle of hepatitis B virus. J Hepatol 2013;59:934–941.

55. Baghaei K, Tokhanbigli S, Asadzadeh H, Nmaki S, Reza Zali M, Hashemi SM. Exosomes as a novel cell-free therapeutic approach in gastrointestinal diseases. J Cell Physiol 2019;234:9910–9926.

56. Rydell GE, Prakash K, Norder H, Lindh M. Hepatitis B surface antigen on subviral particles reduces the neutralizing effect of anti-HBs antibodies on hepatitis B viral particles in vitro. Virology 2017;509:67–70.

57. Mason A, Wick M, White H, Perrillo R. Hepatitis B virus replication in diverse cell types during chronic hepatitis B virus infection. Hepatology 1993;18:781–789.

58. Sukriti S, Choudhary MC, Maras JS, Sharma S, Thangariyal S, Singh A, Das S, Islam M, Sharma S, Trehanpati N, Gupta E, Sarin SK. Extracellular vesicles from hepatitis B patients serve as reservoir of hepatitis B virus DNA. J Viral Hepat 2019;26:211–214.

59. Dejean A, Lugassy C, Zafrani S, Tiollais P, Brechot C. Detection of hepatitis B virus DNA in pancreas, kidney and skin of two human carriers of the virus. J Gen Virol 1984;65(Pt 3):651–655.

60. Kong D, Wu Di, Wang T, Li T, Xu S, Chen F, Jin X, Lou G. Detection of viral antigens in renal tissue of glomerulonephritis patients without serological evidence of hepatitis B virus and hepatitis C virus infection. Int J Infect Dis 2013;17:e535–e538.

61. Bruns M, Miska S, Chassot S, Will H. Enhancement of hepatitis B virus infection by noninfectious subviral particles. J Virol 1998;72:1462–1468.

62. Ladner SK, Otto MJ, Barker CS, Zaifert K, Wang GH, Guo JT, Seeger C, King RW. Inducible expression of human hepatitis B virus (HBV) in stably transfected hepatoblastoma cells: a novel system for screening potential inhibitors of HBV replication. Antimicrob Agents Chemother 1997;41:1715–1720.

63. Gripon P, Rumin S, Urban S, Le Seyec J, Glaise D, Cannie I, Guyomard C, Lucas J, Trepo C, Guguen-Guillouzo C. Infection of a human hepatoma cell line by hepatitis B virus. Proc Natl Acad Sci U S A 2002;99:15655–15660.

64. Heermann KH, Goldmann U, Schwartz W, Seyffarth T, Baumgarten H, Gerlich WH. Large surface proteins of hepatitis B virus containing the pre-s sequence. J Virol 1984;52:396–402.

65. Deng L, Jiang W, Wang X, Merz A, Hiet M-S, Chen Y, Pan X, Jiu Y, Yang Y, Yu B, He Y, Tu Z, Niu J, Bartenschlager R, Long G. Syntenin regulates hepatitis C virus sensitivity to neutralizing antibody by promoting E2 secretion through exosomes. J Hepatol 2019;71:52–61.

66. Tokuyasu KT. A technique for ultracryotomy of cell suspensions and tissues. J Cell Biol 1973;57:551–565.

67. Liou W, Geuze HJ, Slot JW. Improving structural integrity of cryosections for immunogold labeling. Histochem Cell Biol 1996;106:41–58.

68. Griffiths G. Fine structure immunocytochemistry. Springer Science & Business Media, 2012.

69. Hajibagheri MN. Electron microscopy: methods and protocols. Springer Science & Business Media, 1999.

70. Oorschot V, de Wit H, Annaert WG, Klumperman J. A novel flat-embedding method to prepare ultrathin cryosections from cultured cells in their in situ orientation. J Histochem Cytochem 2002;50:1067–1080.

Correspondence
Address correspondence to: Prof. Dr. Eberhard Hildt, Paul-Ehrlich-Institut, Virology, Paul-Ehrlich-Str 51-59, 63225 Langen, Germany. e-mail: eberhard.hildt@pei.de.

CRediT Authorship Contributions

Qingyan Wu (Conceptualization: Equal; Formal analysis: Lead; Investigation: Lead; Methodology: Equal; Visualization: Lead; Writing – original draft: Lead)

Mirco Glitscher (Investigation: Equal; Methodology: Equal; Visualization: Equal)

Susanne Tonnemacher (Data curation: Supporting; Methodology: Supporting)

Anja Schollmeier (Formal analysis: Supporting; Investigation: Supporting; Methodology: Supporting)

Jan Raupach (Investigation: Supporting; Methodology: Supporting)

Tobias Zahn (Formal analysis: Supporting; Methodology: Supporting)

Regina Eberle (Methodology: Supporting)

Jacomine Krijnse-Locker (Methodology: Supporting)

Michael Basic (Methodology: Supporting)

Eberhard Hildt, Prof Dr (Conceptualization: Lead; Formal analysis: Equal; Funding acquisition: Lead; Resources: Lead; Supervision: Lead; Writing – review & editing: Lead)

Conflicts of interest

The authors disclose no conflicts.

Funding